fire

MDPI

Article

Compartment Fire Behavior at the Stages of Detection, Containment and Suppression Using Water Mist

Geniy Kuznetsov [1,*], Roman Volkov [2], Aleksandr Sviridenko [1] and Alena Zhdanova [2]

[1] School of Energy and Power Engineering, National Research Tomsk Polytechnic University, 634050 Tomsk, Russia
[2] Research School of High-Energy Physics, National Research Tomsk Polytechnic University, 634050 Tomsk, Russia
* Correspondence: kuznetsovgv@tpu.ru

Abstract: This paper presents experimental research findings regarding the characteristics of fire safety equipment activation before and after a water-based fire suppression system is triggered. A group of typical indoor combustible materials (wood, linoleum, cardboard, paper) were used to construct Class A model fires in the experiments. The three most frequent fire causes were reproduced: the careless handling of fire (open flame), the unsafe operation of heating equipment and electrical short circuits. To identify the fire behavior, an automated system including fire (heat, smoke, flame) detectors, contact and non-contact temperature measurement instruments, a gas analysis system and video recording equipment was employed. Following the experiments, the most efficient (in terms of detection speed and reliability) combinations of technical equipment that are necessary and sufficient to identify all the combustion stages of substances and materials were determined. The efficient consumption of a fire-extinguishing agent was found to be possible when fire development stages were controlled. Guidelines on creating automated fire prevention systems in buildings were provided. These have the potential to significantly speed up compartment fire suppression.

Keywords: compartment fires; ignition; pyrolysis; flame combustion; detection; different fire hazard sources

Citation: Kuznetsov, G.; Volkov, R.; Sviridenko, A.; Zhdanova, A. Compartment Fire Behavior at the Stages of Detection, Containment and Suppression Using Water Mist. *Fire* **2022**, *5*, 155. https://doi.org/10.3390/fire5050155

Academic Editors: Guan-Yuan Wu, Chao Zhang, Young-Jin Kwon and Nugroho Yulianto Sulistyo

Received: 30 August 2022
Accepted: 27 September 2022
Published: 30 September 2022

1. Introduction

Compartment fires lead to disastrous consequences for a number of reasons [1–8]. The main problem is the massive destruction of the structure of buildings and facilities, floor slabs, staircases and passages. The analysis of emergency consequences shows that the financial damage resulting from firefighting system operation is comparable to that from the burnout of materials and substances in buildings [1–5,9]. Thus, it is reasonable to organize the continuous control of fire suppression in buildings and facilities to minimize excessive dousing with a fire extinguishing agent [10–12]. Liu et al. [12] proposed a new predictive model accounting for the characteristics of the droplet flow and thermal interaction of droplets with a high-temperature environment during a fire. Water mist systems are superior to sprinkler systems in terms of fire suppression time and water consumption in the case of centered fires. Sprinkler systems are more effective with large-area fires. It is also necessary to reduce the number of false alarms and the need to restart sensors after firefighting system activation to control the condition of the seat of the fire [13,14]. Flexible adaptive automated systems are required to solve the corresponding problems of monitoring the fire extinguishing process and adjusting fire suppression systems to the fire behavior [15–19]. Such systems [20–24] have both advantages and disadvantages over traditional fire extinguishing technologies when firefighting agents are sprayed until flame combustion and smoldering are fully suppressed [25–27]. The drawbacks are high development costs and the need for a simultaneous use of a wide group of sensors to reliably record the fire behavior [15,28]. The advantages come primarily from the great

opportunities offered by a targeted supply of fire extinguishing agents to different areas of a building, water supply deactivation upon receiving a signal of completed suppression and the automatic management of all the process stages [15–18]. Such systems are often correlated with the ones relying on feedback from the seat of fire [29,30]. Being very expensive, these systems are used, unfortunately, only at dedicated facilities. It is an important task to develop such systems by optimizing the type and number of sufficient sensors with flexible operation algorithms at the stages of fire detection, containment and suppression [29,30].

The combustion characteristics of typical indoor materials and substances vary within wide ranges [2,5,31,32]. The main characteristics include [32] thermal decomposition start temperature, ignition temperature, flash point, fire point, composition of thermal decomposition and combustion products, combustion front spread rates, etc. Thus, it is necessary to reliably determine the type of pyrolyzing or burning material and substance, as well as the combustion zone sizes, in order to improve the fire suppression system performance. The most promising systems to accomplish these objectives include video recording equipment [15,17,18,33] and a gas analysis complex [16,34]. Video recording systems share one common drawback: they are highly sensitive to interferences, which causes false alarms when solar radiation is re-reflected from glass and mirrors. Gas analysis complexes and systems [16,34] usually feature a long response time (from several tens of seconds to several minutes) and limitations on selectivity when detecting particular gases during the combustion of a group of substances and materials. The spraying of a firefighting agent to a combustion zone generates a flow of vapor, smoke and gas–vapor mixture with a complex component composition. These conditions prevent consistent performance of video recording and gas analysis systems. To improve the efficiency of video recording and gas analysis systems, it is necessary to provide special conditions and false alarm elimination throughout fire suppression. Under such conditions, it is reasonable to use specialized data processing algorithms and additional sensors. Such algorithms serve to manage a complex of gas analysis systems, thermocouple trends and a visualization system, adapted to the research objectives. Relying on a minimal set of input data (e.g., SD readings and gas analysis system data), the algorithm must ensure an early detection of a fire, accurate identification of the type of combustible material in the fire and prediction of the suppression parameters (type of fire-extinguishing agent and its application method) based on the experimental results. Xiong et al. [35] proposed a technology of estimating the fire sizes, shape and location based on the attenuation of the alarm sound. Using this monitoring technology [35] as part of modern fire detection systems can significantly improve their efficiency. At the same time, it is important to suggest engineering solutions with a minimum number of sensors and hence cost. The research findings [14] indicate that the choice of an effective sensor or a group of sensors is mainly conditioned by the type of combustible material. Significantly, Zhdanova et al. [14] investigated the specific aspects of fire sensor operation when there was an open flame, i.e., when a fire already broke out (in terms of real-life conditions). Thus, it is necessary to compare the fire warning sensor performance characteristics in buildings when fire suppression systems (most frequently water-based) are activated, using the results of experiments with fires caused by the most commonly recorded ignition sources. This served as the motivation for the research.

The scientific novelty of the research comes from developing an approach for early detection of a potential fire at the stage when the thermal decomposition of the material begins. The manuscript demonstrates how to identify the start of thermal decomposition and type of material to make prompt decisions for quick fire suppression. The purpose of the research is to determine an effective combination of sensors to minimize false alarms, ensure timely set-off and deactivation of water-based fire suppression when the most typical indoor materials are on fire.

2. Materials and Properties

The experiments involved class A model fire burning and suppression. Combustible materials characteristic of most indoor (residential, warehouse, business) spaces were used to construct model fires [36–38]. Pine wood (density 520 kg/m^3 at a humidity of 12–15%; heat of combustion approx. 18 MJ/kg [39,40]) burns to produce a water steam, carbon dioxide and monoxide, aldehydes, acids and different gases. Fabric backed linoleum (polyvinyl chloride with plasticizers, fillers and dyes) does not support active combustion. Active combustion implies a process when a combustible material continues supporting flame combustion without any external thermal impact. The main combustion product of polyvinyl chloride is hydrogen chloride. Corrugated cardboard consists mainly of recycled materials (semicellulose, straw, waste paper, etc.), the rest being primary cellulose fibers. Class A paper (the density according to ISO is 80 g/m^2, approx. 800 kg/m^3) burns to produce carbon dioxide and monoxide, as well as water steam.

The model fire area, S_f, in the conducted experiments was varied between 5 and 300 cm^2 and the mass of materials to be burned m_f was 2.5–90 g. These ranges are sufficient to extrapolate the research findings to seats of fire of different sizes (with $S_f > 1$ m^2). The final S_f and m_f were conditioned by the type of material and specific aspects of ignition (temperature of combustion and smoldering, burnout rate, heat release and heat release rate), containment (possibility of self-extinguishing when flame combustion is contained) and suppression (necessary water volume and fire-extinguishing agent application time) of fires.

3. Experimental Technique

Three most common causes of compartment fires were considered in the experimental research [5]. Potential fire hazard sources in the experiments were simulated using a gas burner (corresponding to careless handling of fire, an open flame), an inverter welder (corresponding to improper use of electrical equipment and networks, electrical short circuit) and a hot plate (corresponding to unsafe operation of heating equipment, heating materials to high temperatures). The main characteristics of the equipment in use are as follows: a gas burner (using a mixture of combustible gases such as propane and butane for fuel; flame height 50–120 mm; maximum flame temperature approx. 1000 °C); a hot plate (maximum power 1000 W; hot surface diameter 155 mm; maximum surface temperature 550 °C); a welder (inverter type; output short-circuit current 20–140 A; electrode diameter 2 mm).

Figures 1 and 2 present the layout and appearance of the experimental hardware and software system and its main elements. The experimental system featured a set of elements and devices to produce a physical model of the initial stage of a compartment fire. It was used to determine the characteristics of detection, containment and suppression of fires involving combustible materials typical of closed spaces. Three types of experiments imitating the fire causes specified above were carried out. Class A model fires composed of typical indoor combustible materials were used (Section 2).

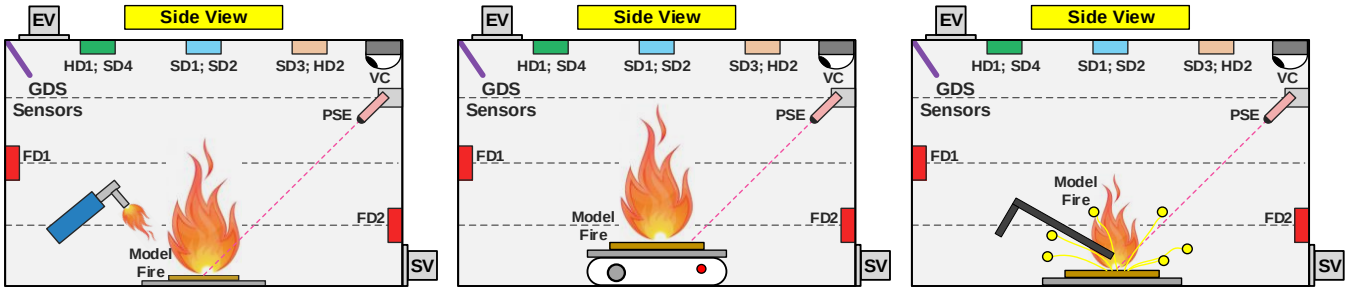

Figure 1. Setup layout illustrating three different ways used to start a model fire burning (heat detector–HD, smoke detector–SD, video camera–VC, pyrometer sensing element–PSE, flame detector–FD, gas detection system–GDS, exhaust ventilation–EV, supply ventilation–SV).

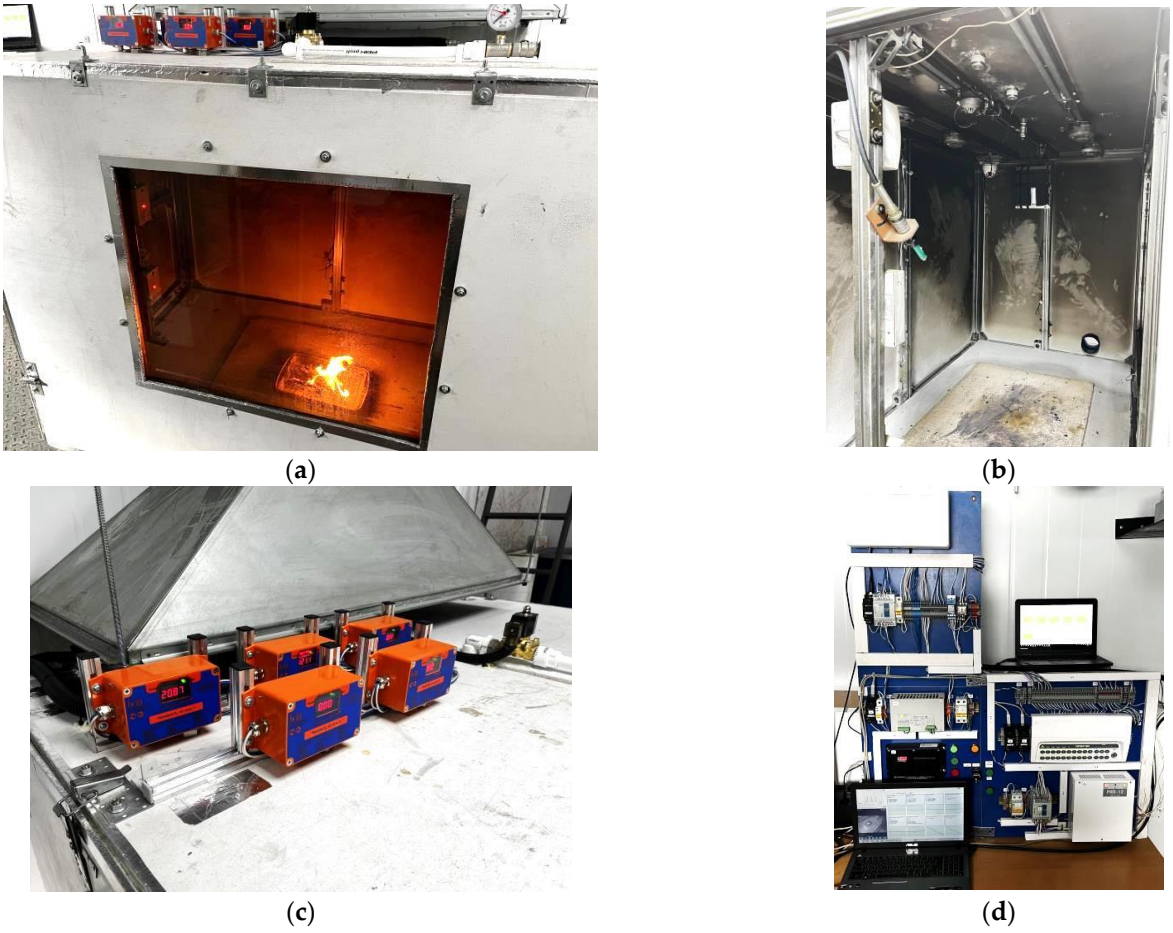

Figure 2. Appearance: (**a**) of the setup exterior; (**b**) of the inner part of the setup; (**c**) of the gas analysis system; (**d**) of the control panel for data collection and fire suppression control.

The experimental system (Figure 2) consisted of a fire-resistant body, a distribution board, recording devices (digital and analog input module–DAIM, fire alarm control device–FACD), technical equipment (thermocouples–TC, high-speed pyrometer, GDS, FD, HD, SD, VC) and a PC to collect and record information about the characteristics of ignition and fire extinguishing, as well as to receive signals from fire detectors fitted inside the fire-resistant setup body. The fire-resistant setup (Figure 2) was a hollow cuboid with the dimensions 1.5 × 1 × 1.25 m (D × W × H). Its side walls were 10-mm-thick fire-resistant magnesium oxide boards. The setup framework was assembled with aluminum beams 45 × 45 mm in square section. An observation window made of 4-mm-thick fire-resistant glass was on one of the side walls. Its dimensions were 0.7 × 0.8 m (Figure 2b). To remove smoke from the setup chamber, it had cylinder-shaped supply (SV) and exhaust ventilation (EV) ducts 120 mm in diameter. The SV duct was installed in the lower part of the setup side wall. On the opposite side, the EV duct was in the upper part of the setup (Figure 2b,c). To prevent the air inflow and combustion product outflow during the experiments, the SV and EV ducts were additionally fitted with sealing gate valves. Inside the experimental setup, there were (Figure 2b,c) point-type detectors (FD, HD, SD, TC) to identify the fire behavior and moment of fire outbreak, GDS sensors to control the component composition of products resulting from the thermal decomposition and oxidation of combustible materials, a sensitive optical element of a high-speed heat-resistant industrial pyrometer (PSE) to measure the model fire surface temperature, a VC to capture the images of model fire burning and suppression, as well as a nozzle with a water supply duct to contain and suppress a fire. A model fire is a fire with a controlled composition, mass of materials, area, temperature and mechanism of ignition.

Signals from point-type fire detectors (FD, HD, SD) and from the high-speed pyrometer (PSE) were transmitted to the distribution board (Figure 2d) complete with a set of electric devices (pyrometer processor unit–PPU, FACD, DAIM) to display data from fire detectors, transmit data from the sensors and signals from thermocouples, GDS and PSE to the PC for subsequent recording, as well as to control the electric (solenoid) valve on the fire-extinguishing agent supply duct (before the spray nozzle). The description and specifications of the sensors and technical equipment used in the experiments are given in Table 1.

Table 1. Characteristics of sensors and devices used in the experiments (FD, HD, SD, TC, GDS, PSE+PPU, VC, FACD, DAIM).

Name	Principle of Operation	Specifications
FD Pulsar 1-01S flame detector	Conversion of infrared (IR) radiation of the flame in the sensitive element response range into an electrical signal	Activation delay no more than 4.5 s; field-of-view angle 120°; wavelength range of recorded IR radiation 0.8–1.1 μm
HD IP 101-1A-A1 heat detector	An increase in the current drawn by the sensitive element when the ambient temperature threshold is exceeded	Activation delay with a temperature increase at a rate of 3 °C/min (0.05 °C/s) - 580–820 s, at 30 °C/min (0.5 °C/s) - 58–100 s; minimum activation temperature – 54–65 °C
SD IP 212-141 smoke detector (electro-optical point-type)	A change in the output impedance of the detector due to the dissipation of IR light, generated by the light source, as it passes through smoke particles	Activation delay 5–9 s; operating temperature range −45 … +55 °C
TC DTPK(KhA) OWEN thermocouple	Thermoelectric effect (an increase in emf with an ambient temperature rise)	Type K; measurement range 0–1200 °C; systematic error ±2.5 °C; response time 3 s
PSE+PPU Thermoscope-600-1S (heat-resistant commercial pyrometer)	Conversion of the amplitude of electromagnetic radiation from an object in the IR range into the thermal radiation power	Measurement range 300–1200 °C; accuracy 0.5%; repeatability of measurements 0.25%; resolution 1 °C; response time 50 ms; emissivity factor 0.1–1
VC ESVI IPC-DN2.1 dome camera	–	Frame rate 25 fps; resolution 1280 × 720 pix; day/night mode
FACD Signal-20M, Contact 16GSM (fire alarm control devices)	–	20 inputs of alarm circuit connection; response time no more than 300 ms
DAIM MV110-8A OWEN (discrete and analog input module)	–	8 analog inputs; 16 discrete inputs; input channel sampling time 1 s; error of temperature measurement channel ±0.5%

To measure the concentration of the main pyrolysis and flue gas components (O_2, CO, CO_2, H_2 and CH_4), a gas detection system (GDS) consisting of five fixed gas analyzers such as Senson-SV-5023 was used. The distribution board was fitted with a set of electric devices to collect information from GDS, send the data to the PC for current concentrations of gas components to be displayed, recorded and analyzed. Table 2 presents the main characteristics of GDS sensors. In Table 2, the column "Measurement range" characterizes the limits that each of the GDS sensors can measure. The measured gas concentrations correspond to the specified ranges. When the concentration of some gas exceeds the specified range, the measurement is not performed. The gas analysis system fails to record the value and displays an error message. The mechanism of detectors is based on converting the measured value into a standard current signal in the range of 4–20 mA. The column

"Current output range" illustrates the correlation between the output current signal of each sensor with the concentration. This column is for reference only.

Table 2. Main metrological characteristics of GDS sensors.

Measured Component	Measurement Range	Maximum Permissible Relative Error, δ%	Type of Sensor	Current Output Range
Carbon dioxide CO_2	0.01–5%	±15	Optical	0–5%
Carbon monoxide CO	0.1–300 mg/m^3	±10	Electrochemical	0–320 mg/m^3
Methane CH_4	0.01–2.5%	±10	Thermal conductivity	0–5%
Oxygen O_2	0.1–30%	±5	Electrochemical	0–32%
Hydrogen H_2	0.01–4%	±10	Electrochemical	0–4%

The fire detectors (FD, HD, SD) were connected to the FACD in a two-wire fire alarm circuit. In turn, the FACD transmitted a signal of detector activation through a group of relay outputs to the DAIM. Signals from TC went to the DAIM directly. The UProg software installed on the PC was used to set and select the fire alarm loop operating parameters and control the FACD relay output via RS-485. The Owen Process Manager software was applied for input parameter control, the DAIM real-time sampling, graphical representation and recording of signals from FD, HD, SD and TC. The DAIM was connected to the PC using RS-485 interface. An industrial infrared partial radiation pyrometer (Thermoscope-600-1S) measured the model fire surface temperature in the experiments. The pyrometer consisted of two parts: a sensing element (PSE) and a processor unit (PPU). The PSE withstands the ambient temperature of up to 200 °C. It was fixed in the experimental setup space (Figures 1 and 2) and connected to the PPU by a fiber-optic cable carrying infrared radiation. The temperature measured by the PSE was displayed on the PPU screen and also transmitted to the PC via RS-485, where the data were saved using the Thermoscope-TS_S software. An ESVI IPC-DN2.1 dome camera was installed in one of the upper corners in the setup space (Figure 1). The video camera was connected to the PC using Ethernet cable. The video camera data were viewed and stored using the Xeoma software pre-installed on the PC. The data recorded by the Owen Process Manager, Thermoscope-TS_S and Xeoma software were later analyzed and processed. The data from GDS sensors were transferred to the DAIM and then via the RS-485/USB interface converter to the PC, where they were processed and analyzed.

The cause of fire has a significant effect on the rate of fire development and fire characteristics. To consider this factor, a set of experiments was conducted with a group of typical indoor materials. Several most common fire causes were simulated: careless handling of fire, electrical short circuits and unsafe operation of heating equipment. The characteristics of potential fires and fire sensor performance differed significantly for them. The conditions of thermal decomposition and flame combustion of materials were reproduced with three potential fire hazard sources:

1. Gas burner. A model fire involving combustible material (Section 2) was arranged on a metal pallet (30 × 20 cm in size) placed in the lower part (base) of the setup in the center (Figure 2). A gas burner was applied uniformly over the surface area to set it on fire. The flame application time ranged between 10 and 90 s depending on the fire sizes that were conditioned by the combustible material mass. The flame application time was minimum for paper and maximum for wood.
2. Hot plate. A model fire was arranged on a metal pallet (15 × 15 cm in size). The pallet was placed on the hot plate surface preheated to a certain temperature (T_s). The plate was in the lower part (base) of the experimental setup in its center (Figure 1).
3. Welder. A model fire was arranged on a metal pallet (30 × 30 cm in size), placed in the lower part (base) of the experimental setup in its center (Figure 1). The necessary short-circuit current was set at the inverter outlet. A short contact of the welder

electrode with the metal pallet led to the local heating and spark emission, as it occurs during the short circuit of a transmission line.

For each type of combustible material and ignition scheme, two types of experiments were carried out (with and without a fire suppression system activation). In the first case, the recorded parameters were the surface temperature of materials involved in the model fire (T_f); temperature (T) in different points of the setup space; CO, CO_2 and O_2 concentrations in typical points of the experimental setup space; response delay time (t_D) and specific aspects of fire detector operation during a fire. In the second case, the specific aspects of fire detector operation with feedback in place during fire suppression were additionally recorded along with the model fire suppression time (t_e) and water volumes necessary and sufficient to extinguish the model fire. The model fire surface temperature was measured with a high-speed pyrometer (Figure 1). The pyrometer (PSE+PPU) performed point-type measurements (in some areas of the model fire surface). At the same time, the temperature may differ greatly in different points of the model fire surface. Before the experiments, a set of test measurements employing a Testo–885 thermal imager was performed to record the model fire surface temperature. After that, the data from a set of experiments and from test measurements were compared. The comparison showed that the average difference in the values was no more than 5–10%. Therefore, it is safe to say that a high-speed pyrometer provides data on the average temperature of the model fire surface with an accuracy of 5–10%.

A commercially available FMT-100 nozzle generating a polydisperse droplet jet (resembling water mist) with droplet radii in the range of 5–120 μm was used to put out the model fire in the experiments. The nozzle was placed in the upper central part of the experimental setup space (Figure 1b,c) above the model fire. The average specific discharge density of the FMT-100 nozzle was $\psi \approx 0.03$ L/(m^{2}s) or 1.8 mm/min. Discharge density values were selected from preliminary experiments and fire behavior, as well as based on the analysis of research findings and sprinkler system requirements [12,17,41]. Tap water supplied to the spray nozzle through a flexible hose under 200 kPa was used as a fire extinguishing agent. A solenoid valve fitted before the spray nozzle was controlled remotely from the distribution board. Notably, this research did not aim to determine the optimal (in terms of the fire suppression efficiency) match between a combustible material and a fire suppression device or agent. In this study, only a water mist system was employed, as it is the most available and popular one in actual practice [12,41]. There are studies into fire suppression characteristics when other systems are employed, e.g., using slurries, solutions, emulsions, foams, etc. [42–44]. The findings [44] indicate that effective (in terms of suppressing fires with a minimum firefighting agent consumption volume) values of the specific discharge density vary in the range of 0.1–1.6 L/(m^{2}s). Significantly, adding a foaming agent or a wetting agent to a combustible material may both decrease and increase the specific discharge density. Therefore, the selection of an effective firefighting agent for each type of combustible material is obviously the topic of a separate full-scale study.

The start of fire suppression depended on the heating scheme being used and specific aspects of pyrolysis and combustion of the material:

- gas burner. Extinguishing started after the fire surface temperature (measured by the PSE) reached constant values (fluctuations in T_f were no more than ± 50 °C) or when at least two fire detectors were triggered. Water was sprayed as long as smoldering continued (recorded by the VC readings) and until the temperature T_f fell below 200 °C (corresponds to the average temperature at which the thermal decomposition of the considered materials began);
- hot plate. Due to the absence of flame combustion (in most cases), fire was extinguished when two fire detectors (usually SD) were triggered. Water was normally sprayed until smoke generation completely stopped and as long as there was smoldering (recorded by the VC readings);

- welder. Fire suppression started when two fire detectors were triggered. Water spraying continued until smoke generation completely stopped and as long as there was smoldering (recorded by the VC readings).

In the research, additional experiments were carried out to evaluate the effect of fine water mist inside the experimental setup on the characteristics (intensity) of VC images. To that end, a commercial ultrasonic water mist maker (air humidifier) was used: number of ultrasonic membranes–10; water flow rate–4.5 L/h; size (diameter) of generated droplets–2–5 μm. The water mist generated by the humidifier was supplied through a flexible duct (50 mm in diameter) into the experimental setup space through the SV opening. Water mist was supplied for 10 min. Throughout this period, the images of the setup from the inside were recorded by the VC installed in it. The images were then processed (Section 4.3).

Significantly, the suppression characteristics are affected by the room volume, namely, the ceiling height, which normally corresponds to the height of the nozzle placement. The height of ceilings and, thus, the height of nozzle placement primarily influence the velocity of fire extinguishing agent droplets in the region of their interaction with high-temperature combustion products yielded by a fire. The velocity of droplets in the region where they mix with combustion products will also depend on the atomizer characteristics, droplet sizes, pressure in the liquid supply systems and many other factors. Previous studies [45,46] show that when the initial velocity (before the interaction with combustion products) of water droplets is about 3 m/s, they may cover from 0.05 m to 0.3 m in the course of their interaction with combustion products until they completely stop and turn around. Thus, in addition to the research findings presented in this paper, the criterial equations proposed and described in [45,46] can be used to predict the fire suppression efficiency using the sizes and velocities of droplets in a potential fire area. If the calculations predict a turnaround and entrainment of droplets with combustion products, suppression can be considered inefficient, and vice versa.

4. Results and Discussion

Figures 3–5 show typical images of class A model fires (with four materials considered in the research), when simulating different causes of compartment fires (Table 1). The videograms of the conducted experiments are presented in Supplementary Materials A–H.

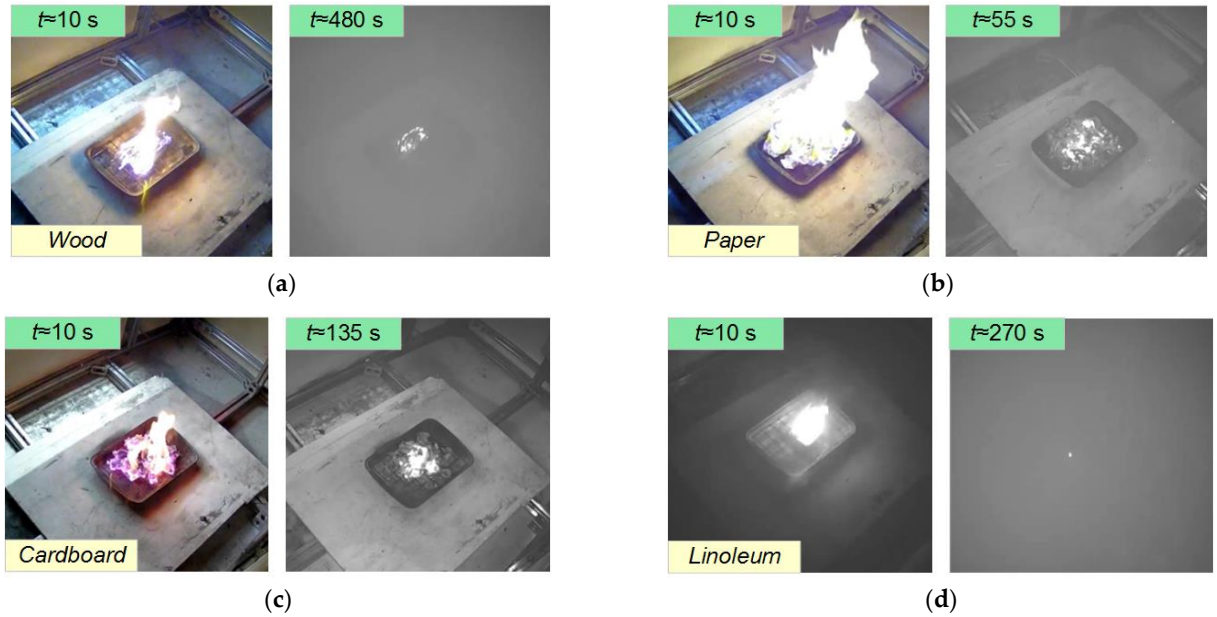

Figure 3. Images of model fire when reproducing conditions of careless handling of fire (gas burner) at the stages (from left to right) of ignition, rapid flame combustion, smoldering start and smoldering completion: (**a**) wood; (**b**) paper; (**c**) cardboard; (**d**) linoleum.

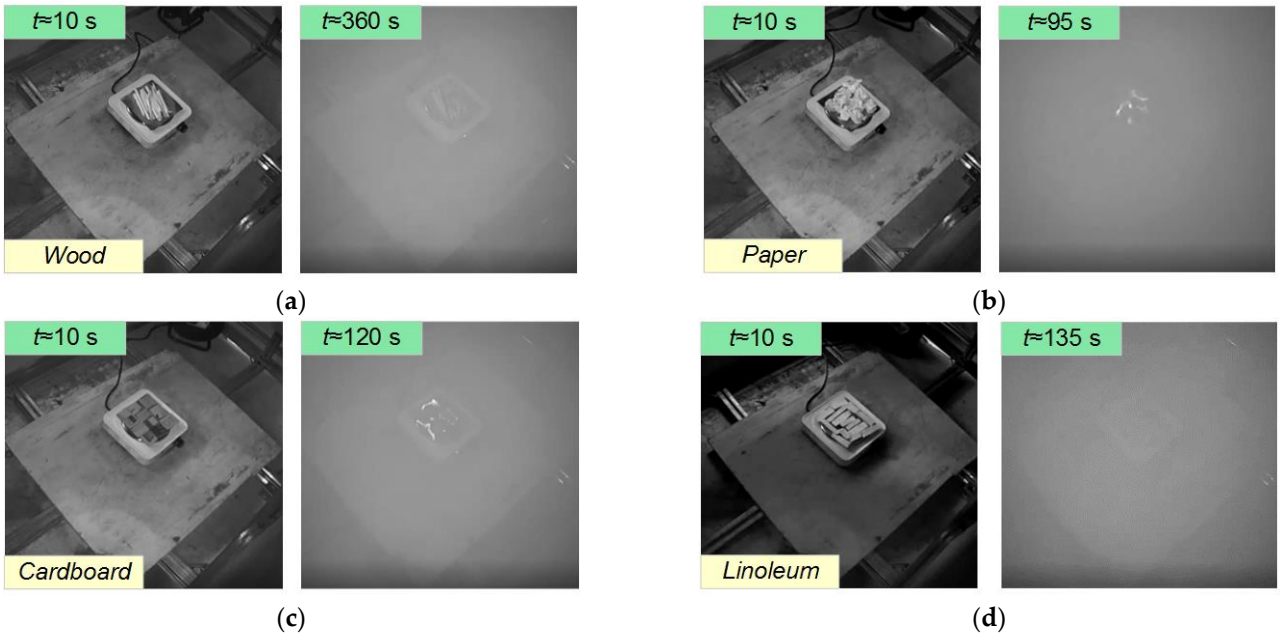

Figure 4. Images of model fire when reproducing conditions of unsafe operation of heating equipment (hot plate) at the stages (from left to right) of heating, pyrolysis start and rapid smoke generation: (**a**) wood; (**b**) paper; (**c**) cardboard; (**d**) linoleum.

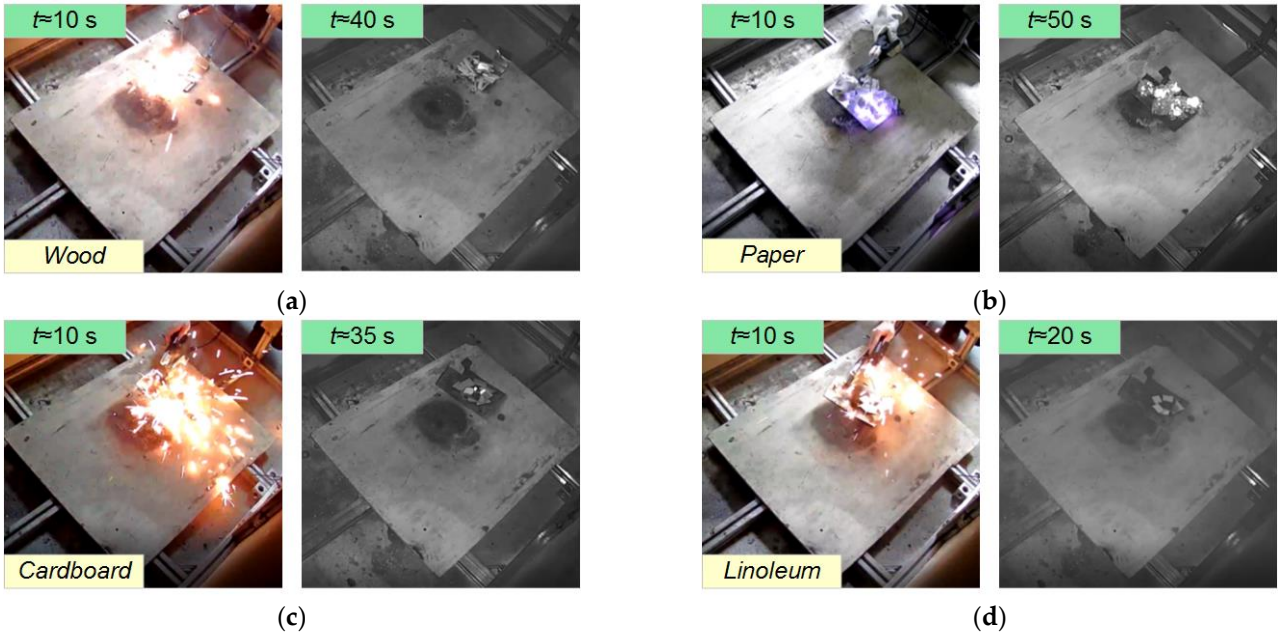

Figure 5. Images of model fire when simulating improper use and emergency operation of electrical equipment and networks (electric discharge generation with a welder) at the stages (from left to right) of ignition (short circuit), flame combustion, smoldering and extensive smoke generation: (**a**) wood; (**b**) paper; (**c**) cardboard; (**d**) linoleum.

Following the conducted experiments, specific aspects of combustion of the considered materials were identified when reproducing compartment fire causes without a fire suppression system activation:

- gas burner (Figure 3). The model fires involving wood went through the following stages: sustainable flame combustion, prolonged and extensive smoldering, weak smoke generation during flame combustion, more extensive smoke generation during

smoldering. The following stages were recorded for the model fires composed of paper: sustainable flame combustion, short smoldering and weak smoke generation. The stages recorded for the model fires made up of cardboard were sustainable flame combustion, short smoldering and moderate smoke generation (usually at the stage of smoldering). The model fires composed of linoleum went through sustainable flame combustion, short smoldering and extensive smoke generation;

- hot plate (Figure 4). Prolonged smoldering (the intensity depended on the surface temperature T_s) and extensive smoke generation were typical of all the model fires under study. In some cases (at maximum T_s), in model fires involving paper, the combustible material ignited and there was sustainable flame combustion leading to reduced smoke generation intensity;
- electric discharge generation with a welder (Figure 5). For model fires made up of wood, cardboard and linoleum, in some cases (usually at a short-circuit current of more than 100 A), a short circuit was followed by short (10–20 s) local smoldering of combustible materials accompanied by weak smoke generation. No smoldering was recorded at low short-circuit current values (20–80 A). There was no flame combustion with these types of combustible materials within the range of experimental parameters. Model fires involving paper went through sustainable flame combustion (for 30–40 s) right after (2–3 s) a short circuit. It was followed by short smoldering (5–10 s) accompanied by weak smoke generation (within the whole range of short-circuit current values). Thus, a short circuit imitation led the model fire either to active flame combustion, or to short smoldering, which is similar to the experiments with a gas burner and a hot plate. For that reason, subsequent discussion of the findings will focus on imitated careless handling of fire (gas burner) and unsafe operation of heating equipment (hot plate).

4.1. Characteristics of Fire Detector Activation

Figures 6 and 7 show histograms illustrating the SD activation delay times versus the burning material mass, when simulating careless handling of fire (gas burner), obtained from the analysis of the experiments with fire suppression and without a water discharge system activation.

Figures 8 and 9 present the curves of the SD activation delay times versus the hot plate surface temperature and model fire surface area, when simulating unsafe operation of heating equipment (hot plate).

The experiments revealed the maximum (threshold) values of m_f and S_f above which there is no significant change to the fire detector performance characteristics (mainly, t_D) (Figures 6, 7 and 9). A further increase in the mass of materials and model fire area will only affect the volumes of fire extinguishing agents that are necessary and sufficient to contain and suppress a fire (accounting for the water discharge density determined in this study).

Figure 10 presents the delay times and relative frequency of SD activation as a function of the short-circuit current, when simulating improper use and emergency operation of electrical equipment and networks (using a welder). The overall activation frequency of each sensor type was calculated as the arithmetic mean of the sensor activation frequency in each experiment:

$$P = (P_1 + P_2 + \ldots + P_j)/j, \quad (1)$$

where P_1, P_2, . . . , P_j– relative frequency of sensor activation in each experiment, %.

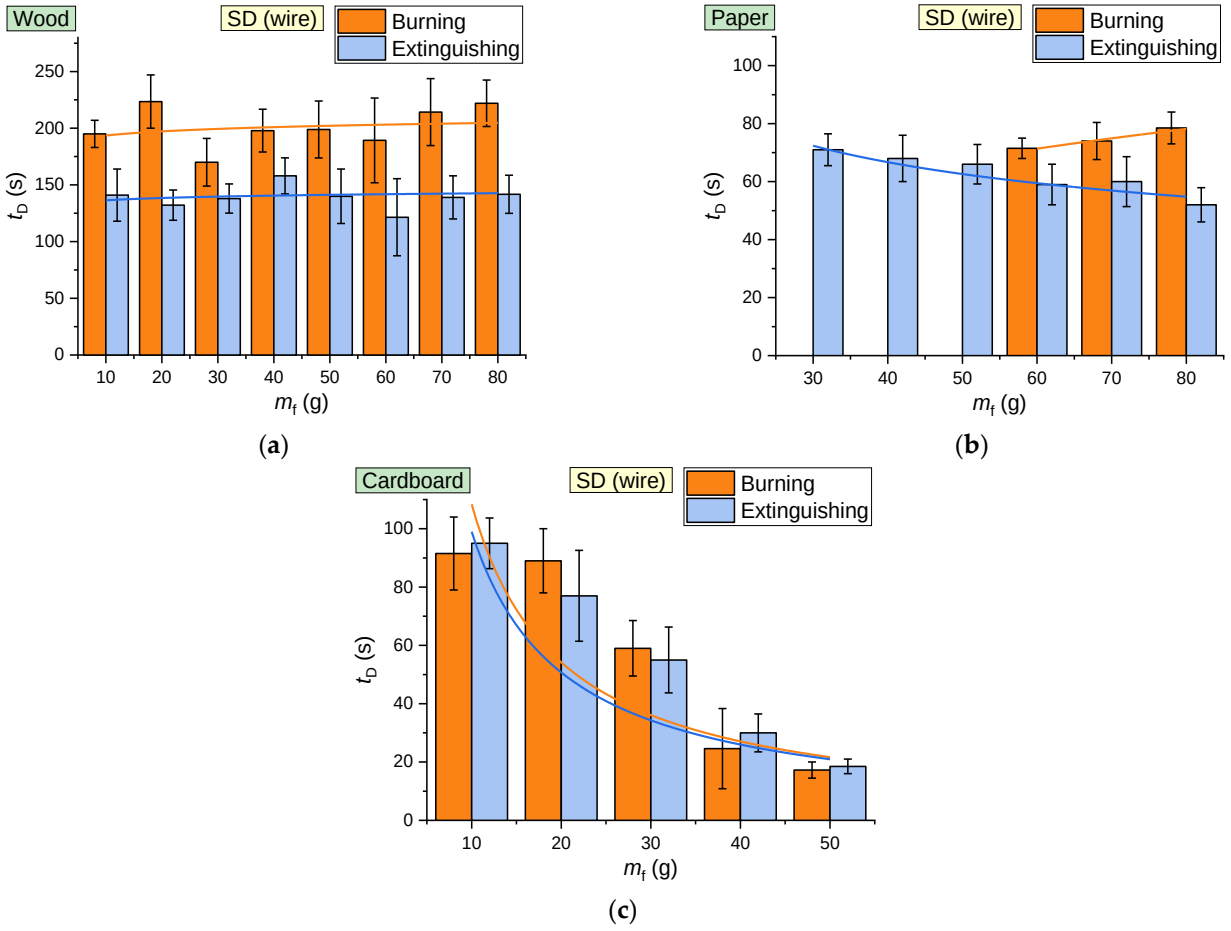

Figure 6. Activation delay times of SD (in the circuit), when varying the sample mass in the experiments with open flame: (**a**) wood; (**b**) paper; (**c**) cardboard.

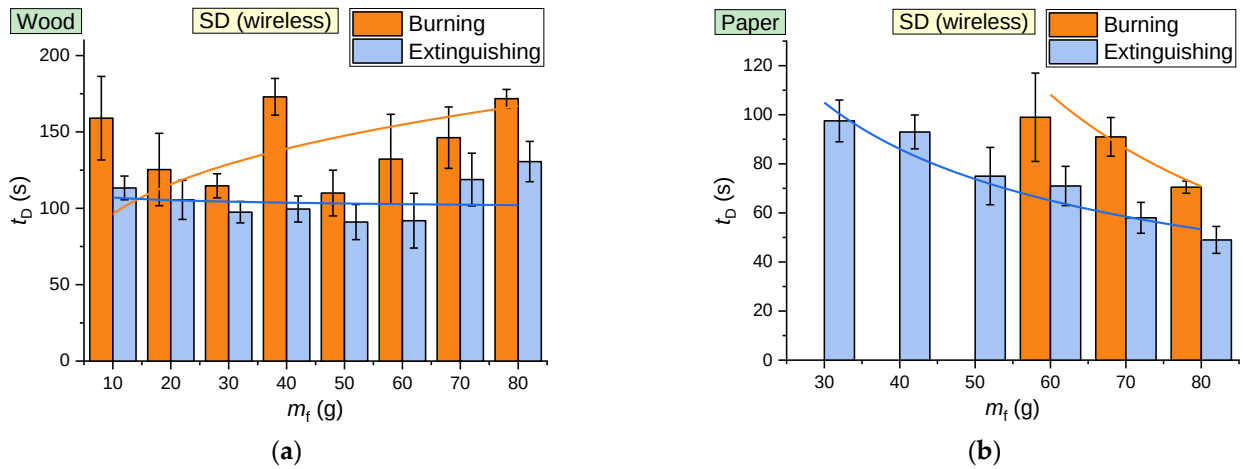

Figure 7. *Cont.*

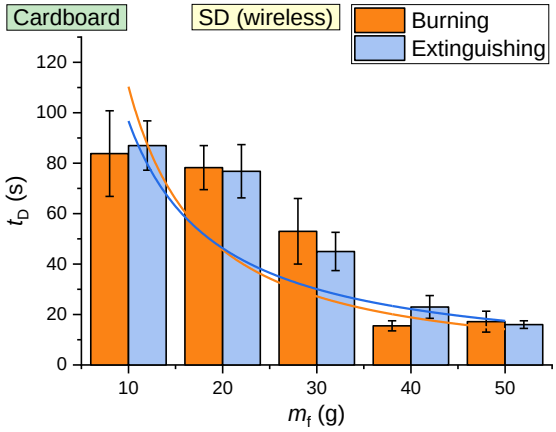

Figure 7. Activation delay times of wireless SD, when varying the sample mass in the experiments with open flame: (**a**) wood; (**b**) paper; (**c**) cardboard.

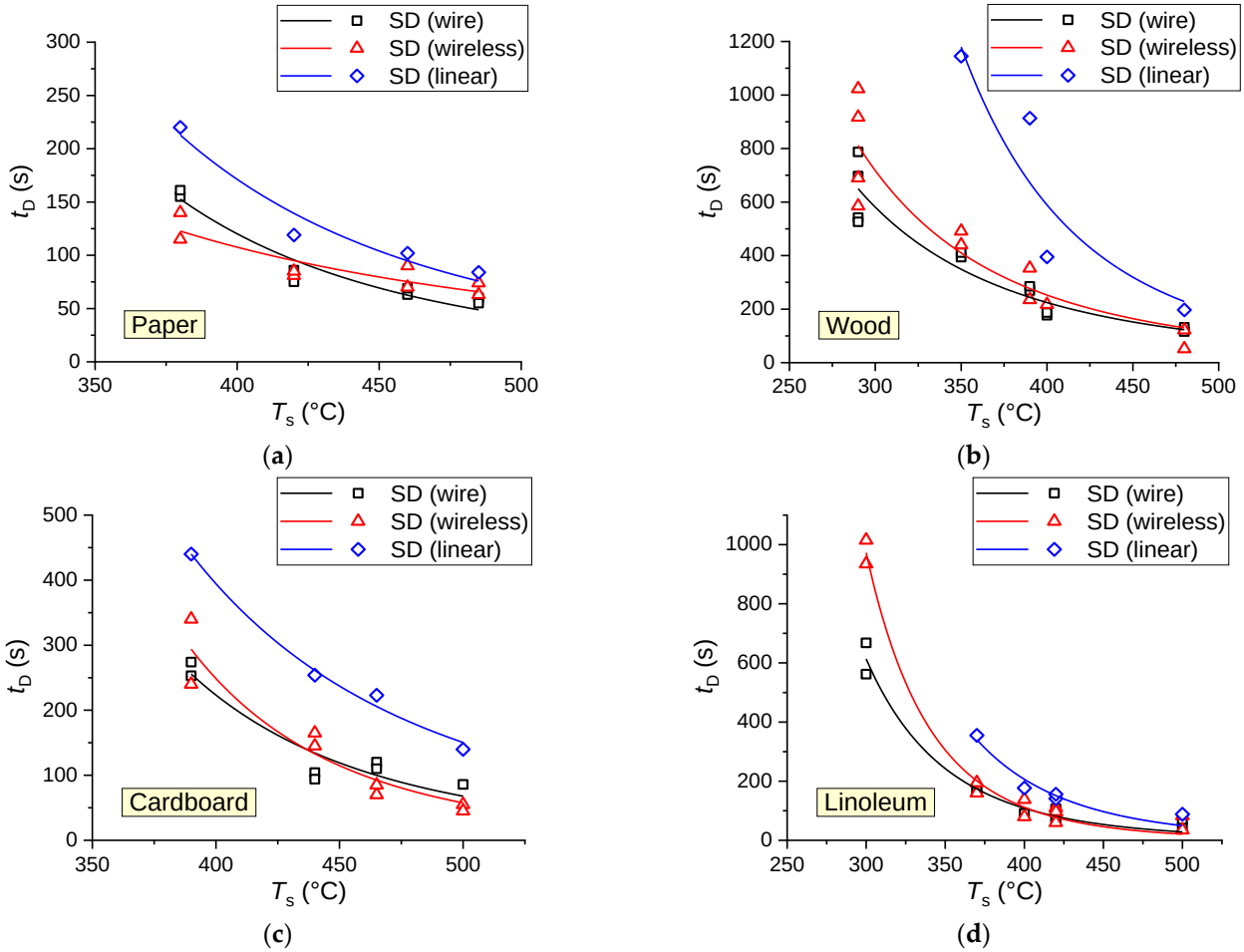

Figure 8. SD activation delay times when varying the hot plate surface temperature using model fires involving paper (**a**), wood (**b**), cardboard (**c**) and linoleum (**d**): SD (wireless) is a wireless smoke detector; SD (wire) is a smoke detector connected in the circuit; SD (linear) is a linear smoke detector.

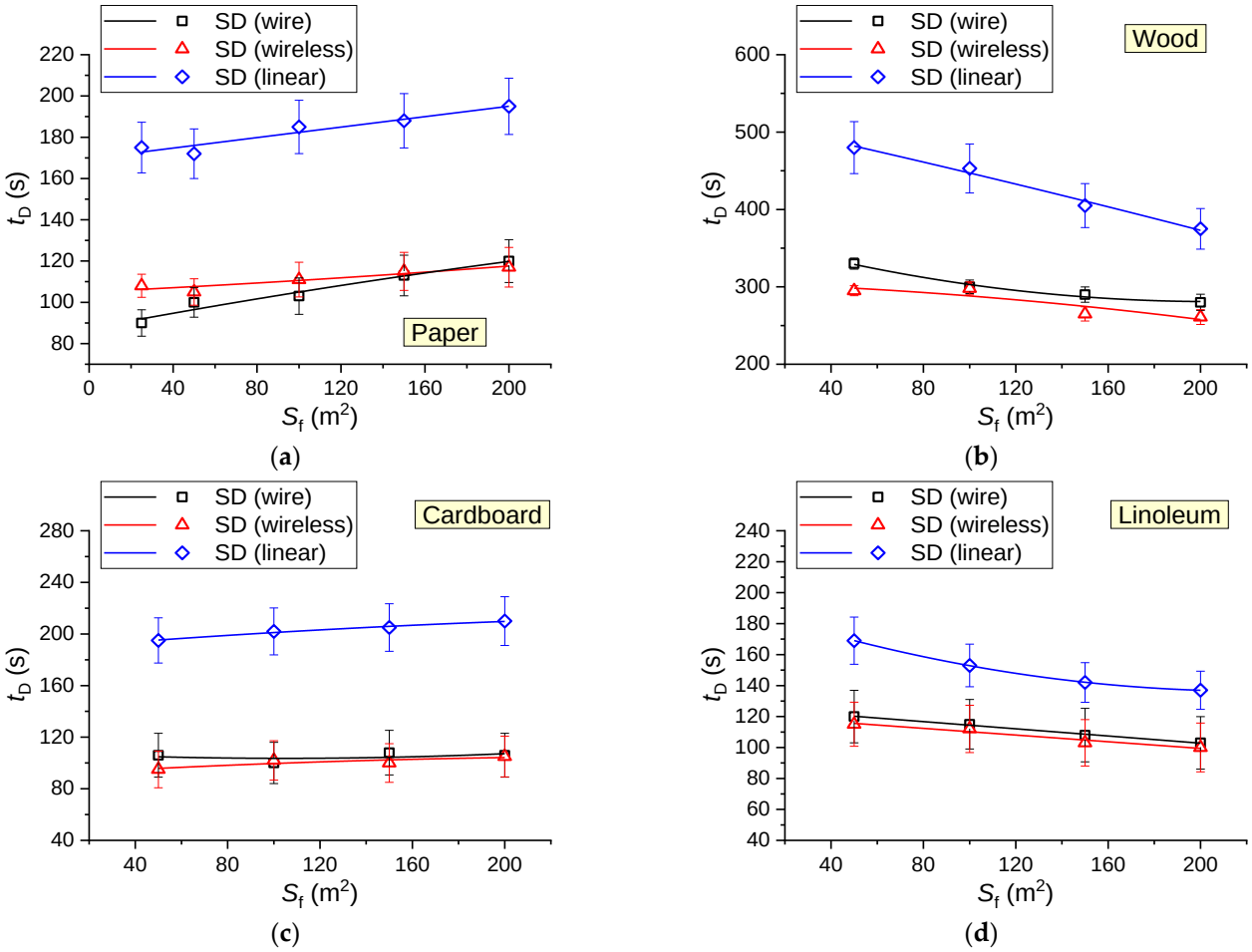

Figure 9. SD activation delay times when varying the area of contact of the fire with the hot plate using model fires involving paper (**a**), wood (**b**), cardboard (**c**) and linoleum (**d**): SD (wireless) is a wireless smoke detector; SD (wire) is a smoke detector connected in the circuit; SD (linear) is a linear smoke detector.

The term "relative frequency" is synonymous to the "activation probability" for sensors. The idea here is the probability of sensor activation, i.e., how many sensors in place were activated. The relative sensor activation frequency in each experiment was calculated as a ratio of the number of activated sensors to the total number of sensors being used:

$$P_j = n_a / n_D, \quad (2)$$

where n_a–number of sensors of a particular type, activated in the experiment; n_D–total number of sensors of a particular type in the experiment.

Figure 11 presents the average delay times and frequency of fire detector activation, when simulating careless handling of fire and improper use of heating equipment for all the model fires under study with and without fire suppression.

Following the analysis of Figure 11, the fire detector efficiency factor (α) was calculated for the imitated fire conditions under study (Figure 12). The parameter α takes two main detector characteristics into account: the activation delay time (time of fire detection) and relative frequency (probability) of activation. The physical significance of the fire detector efficiency factor is that it reflects how reliably and fast a detector is activated in response to fire signs.

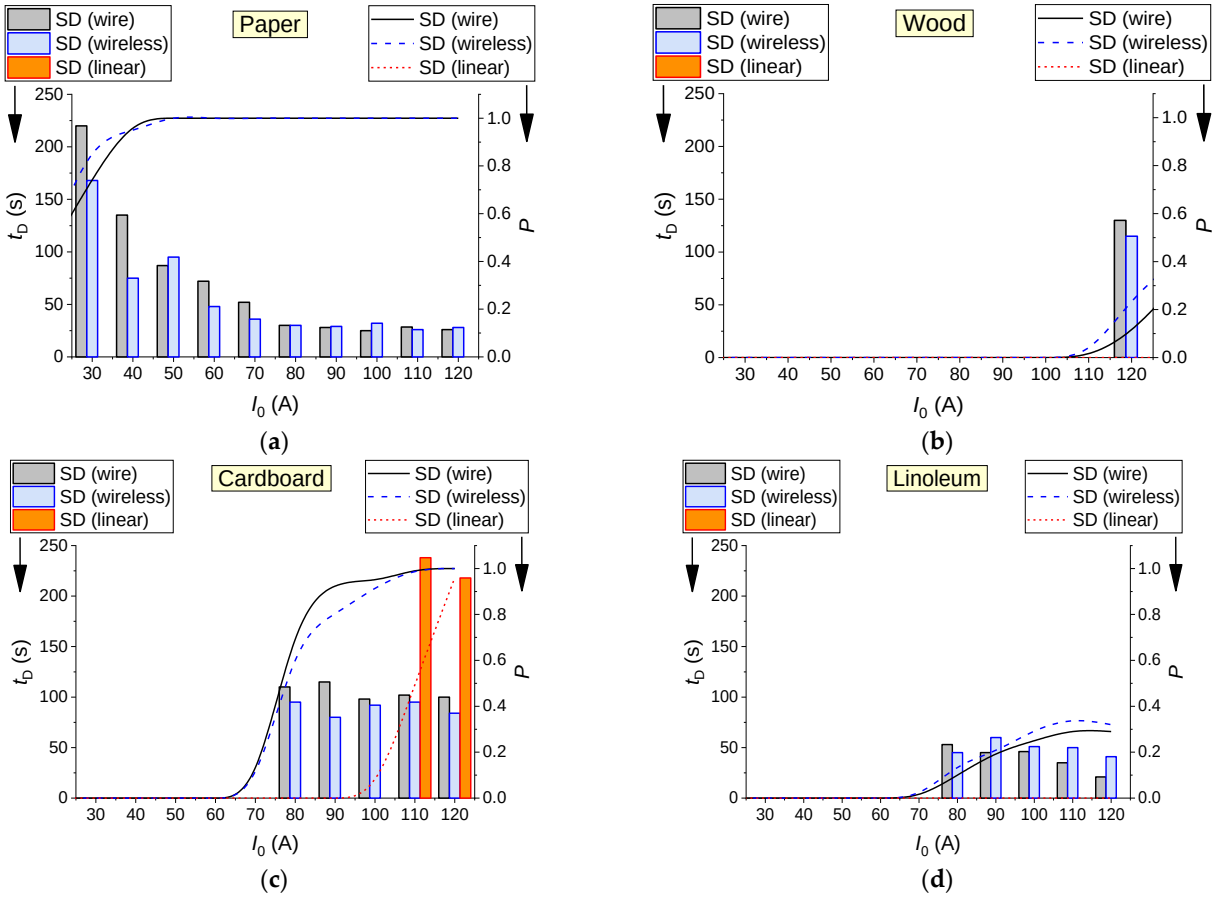

Figure 10. Delay times and frequency of SD activation at different short-circuit current values using model fires composed of paper (**a**), wood (**b**), cardboard (**c**) and linoleum (**d**): SD (wireless) is a wireless smoke detector; SD (wire) is a smoke detector connected in the circuit; SD (linear) is a linear smoke detector.

The value of α was given by

$$\alpha = P \cdot (t_{D(min)} / t_D), \quad (3)$$

where $t_{D(min)}$ is the minimum fire detector activation delay, recorded in the experiments.

Tables 3 and 4 present the SD activation delay times versus the hot plate surface temperature, when simulating unsafe operation of heating equipment without fire suppression and with water application.

Following the analysis of Tables 3 and 4, the main conclusions were drawn:

- it can be seen in Table 3 that an increase in the hot plate surface temperature causes a nonlinear decrease in the SD activation delay times for all the combustible materials (Figure 8). Therefore, it is necessary to install fast-response fire detection sensors in rooms with high-temperature heating systems. In offices, warehouses and residential premises with conventional heating systems, there is no need for a high sensor activation rate;
- an increase in the hot plate surface temperature causes a rapid decrease in the image intensity, which indicates the formation of a high concentration of smoke (filled with solid particles not transmitting light). Such conditions require systems capable of shining brighter light through smoke aerosol when suppressing fires and evacuating people;
- SD activation delay was lowest with model fires consisting of linoleum, paper and cardboard;

- in the experiments with wood at $T_s \approx 290$ °C and linoleum at $T_s \approx 300$ °C, the linear smoke detector was not activated;
- variations in the surface area of contact of a combustible material with a hot surface do not affect the SD activation times or image intensity;
- in the experiments with combustible materials such as paper and cardboard placed in 2–3 layers, the probability of ignition increases;
- smoke detector activation times in the experiments with extinguishing are lower, since smoke concentration increases faster during fire suppression than during constant local heating. SD (linear) is not triggered when burning wood is extinguished.

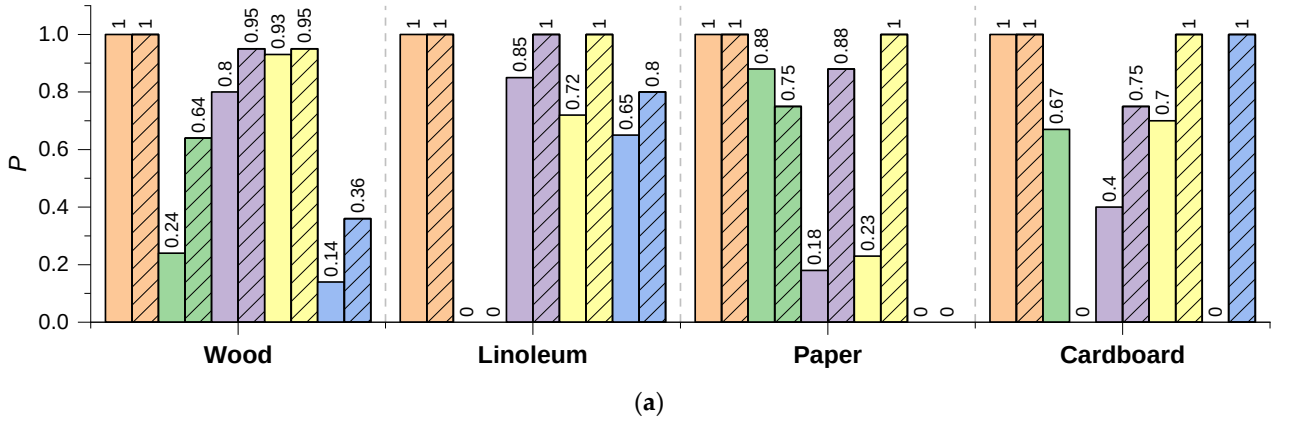

(**a**)

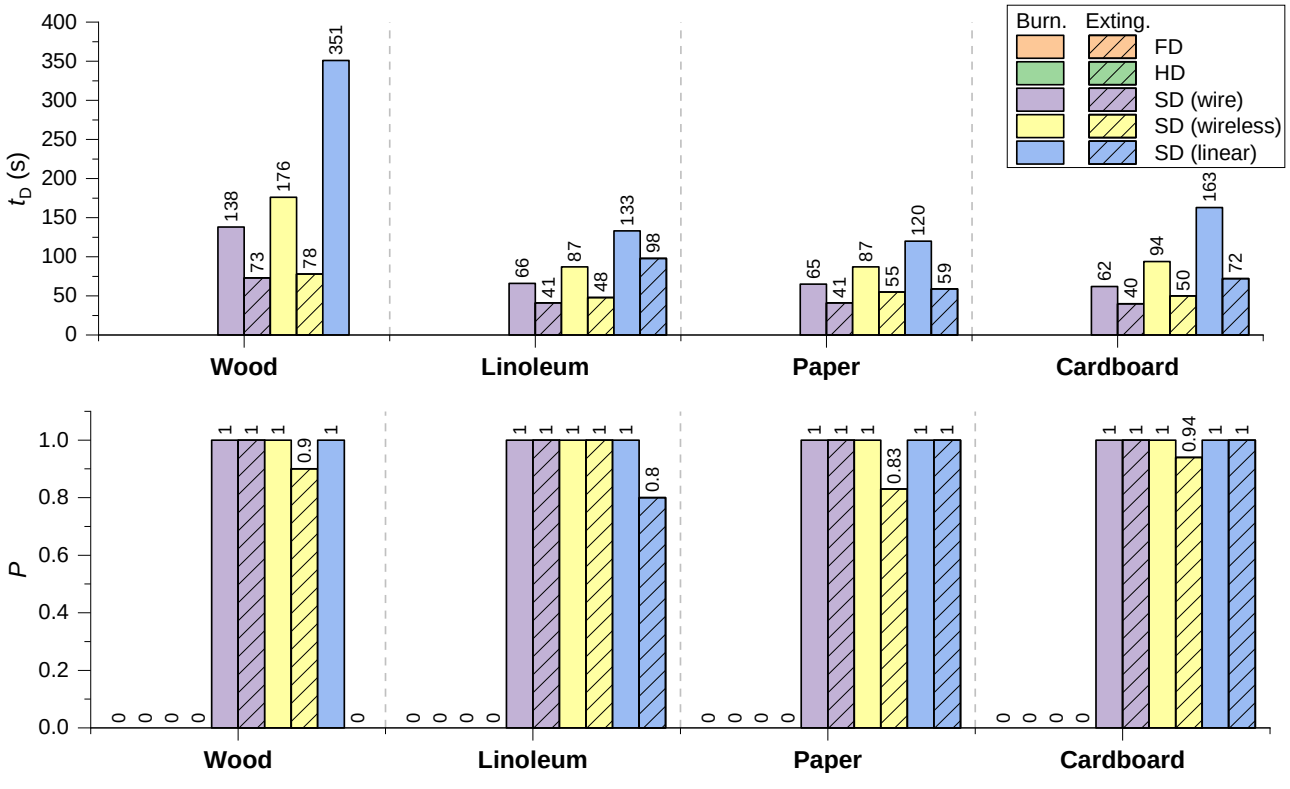

(**b**)

Figure 11. Average delay times and frequency of fire detector activation, when simulating careless handling of fire (**a**) and improper use of heating equipment (**b**) for all the model fires under study with and without water application. SD (wireless) is a wireless smoke detector; SD (wire) is a smoke detector connected in the circuit; SD (linear) is a linear smoke detector; (Burn.–experimental results for the thermal decomposition of the model fire without suppression; Exting.–experimental results for extinguishing the model fire during thermal decomposition).

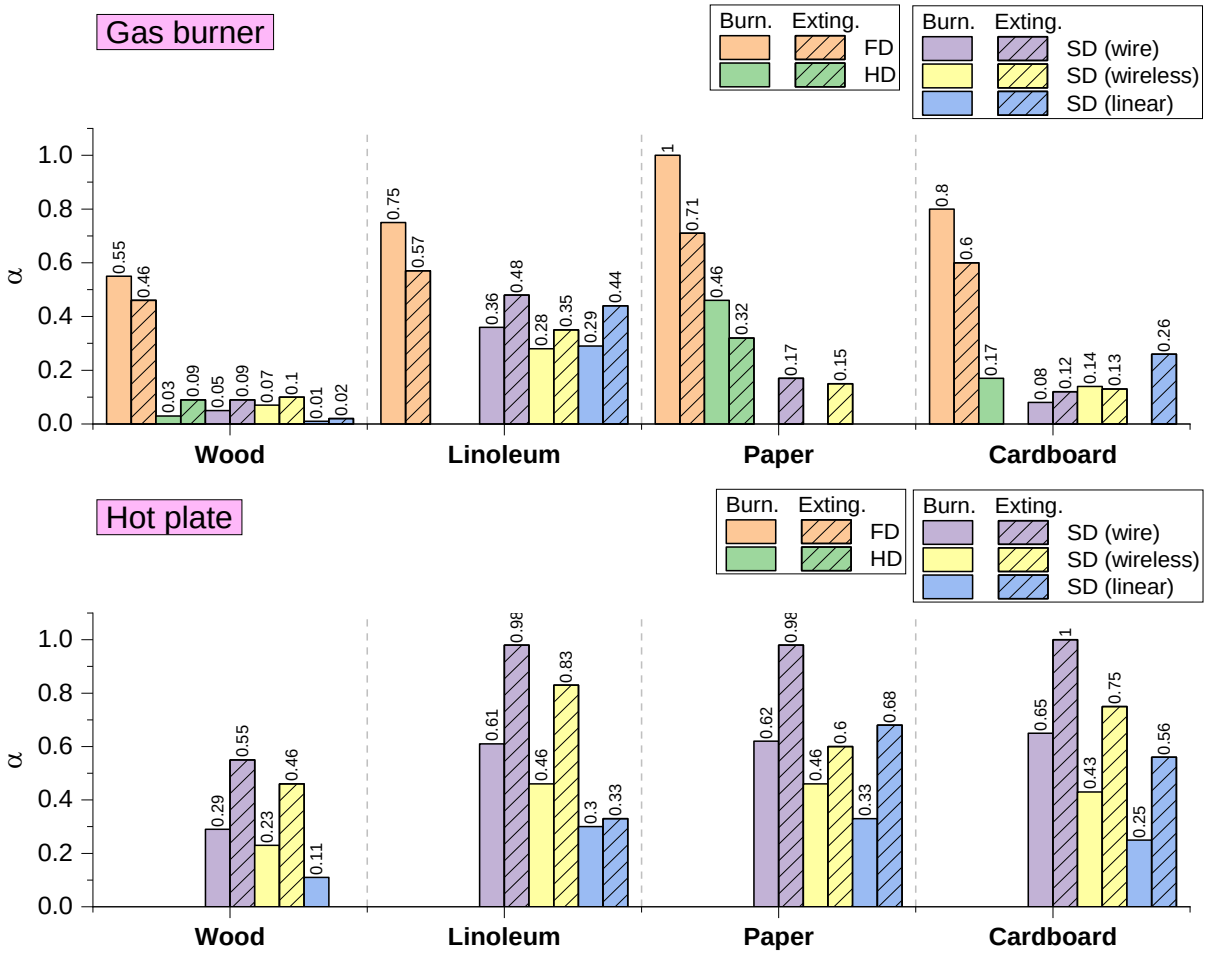

Figure 12. Fire detector efficiency factor when reproducing the conditions of careless handling of fire and improper use of heating equipment for all the model fires under study without extinguishing and with water application.

Table 3. SD activation delay times when varying the hot plate surface temperature under imitated conditions of unsafe operation of heating equipment without fire suppression.

Combustible Material	Hot Plate Surface Temperature, °C	Sensor Activation Delay Time, s	
		SD (Wire, Wireless)	SD (Linear)
Wood	290	628	–
	375	360	1029
	400	240	295
Cardboard	390	299	440
	440	186	244
	483	143	133
Paper	380	190	220
	440	142	90
Linoleum	300	675	–
	370	194	308
	420	157	156
	500	143	80

Some specific patterns were identified, following the conducted experiments (involving different schemes of model fire ignition). First, with a hot plate, flame combustion is not typical of most materials (Figure 4). Extensive pyrolysis usually occurs as a result of

gradual heating of the material. Thus, FD and HD were not activated in these experiments. An increase in the hot plate temperature causes a decrease in the detector activation delay time for all the four combustible materials (Figure 8). At the same time, with changes in the hot plate surface area occupied by the model fire, the SD activation delay time remains almost the same (Figure 9), except for the model fire involving paper. The SD activation delay time increases (Figure 9a) because evenly spread paper releases fewer pyrolysis and combustion products forming the smoke aerosol. Second, with a welder (Figure 5) used to imitate the ignition source, the following aspects should be pointed out. The model fire consisting of wood did not catch fire even at a short-circuit current of approx. 120 A. There was no smoldering or smoke generation in the experiments either (Figure 5a). In certain cases, when the short circuit lasted for more than 3–5 s, some SDs (Figure 10b) were activated, which was caused by rapid electrode heating. The experiments with model fires made up of paper revealed that even a short-circuit current of approx. 20 A was enough to ignite the combustible material and trigger all the SDs except the linear smoke detector (Figure 10a). The linear smoke detector was only activated in the experiments involving cardboard with a current no less than 120 A. Model fires consisting of wood and linoleum required a stronger current to ignite. Thus, at a short-circuit current of 120 A, there was no smoldering or flame combustion. However, when a spark ended up on linoleum, the inflow of thermal decomposition products was sufficient to trigger wired smoke detectors (Figure 10d). Moreover, as it was mentioned above, during a short circuit (usually no more than 3 s), there was smoke released as a result of the metal plate melting, which in some cases led to a short activation of smoke detectors. Third, with a gas burner, there was sustainable flame combustion of all the combustible materials in the experiments (Figure 3). Remarkably, when paper was used in the model fire, its mass had to be at least 80 g for the SD to be activated. This was not the case with the other combustible materials. The flame detector was the first to respond. Table 2 shows the relative frequency (probability) of detector activation.

Table 4. SD activation delay times when varying the hot plate surface temperature under imitated conditions of unsafe operation of heating equipment with extinguishing the fire.

Combustible Material	Extinguishing Time, s	SD Activation Delay Time, s	
		SD (Wire, Wireless)	SD (Linear)
Wood	90	111	–
	60	47	–
	30	62	–
	15	95	–
	5	69	–
Cardboard	120	45	59
	90	49	84
	60	45	73
	30	35	59
Paper	90	42	70
	60	34	44
	30	63	64
Linoleum	60	42	59
	30	49	80
	15	37	76
	10	50	176
	5	45	–

4.2. Component Composition of Combustion Products

Figures S1 and S2 in Supplementary Material S present the trends of O_2, CO, CO_2 and CH_4 concentrations in the experimental setup space, obtained using GDS, for the model fires under study. Careless handling of fire (gas burner) and improper use of heating equipment

(hot plate) were simulated, with and without a fire suppression system activation. Figure 13 compares the trends of CO concentrations over time for all the combustible materials considered in the experiments and two schemes of initiating the thermal decomposition of the material.

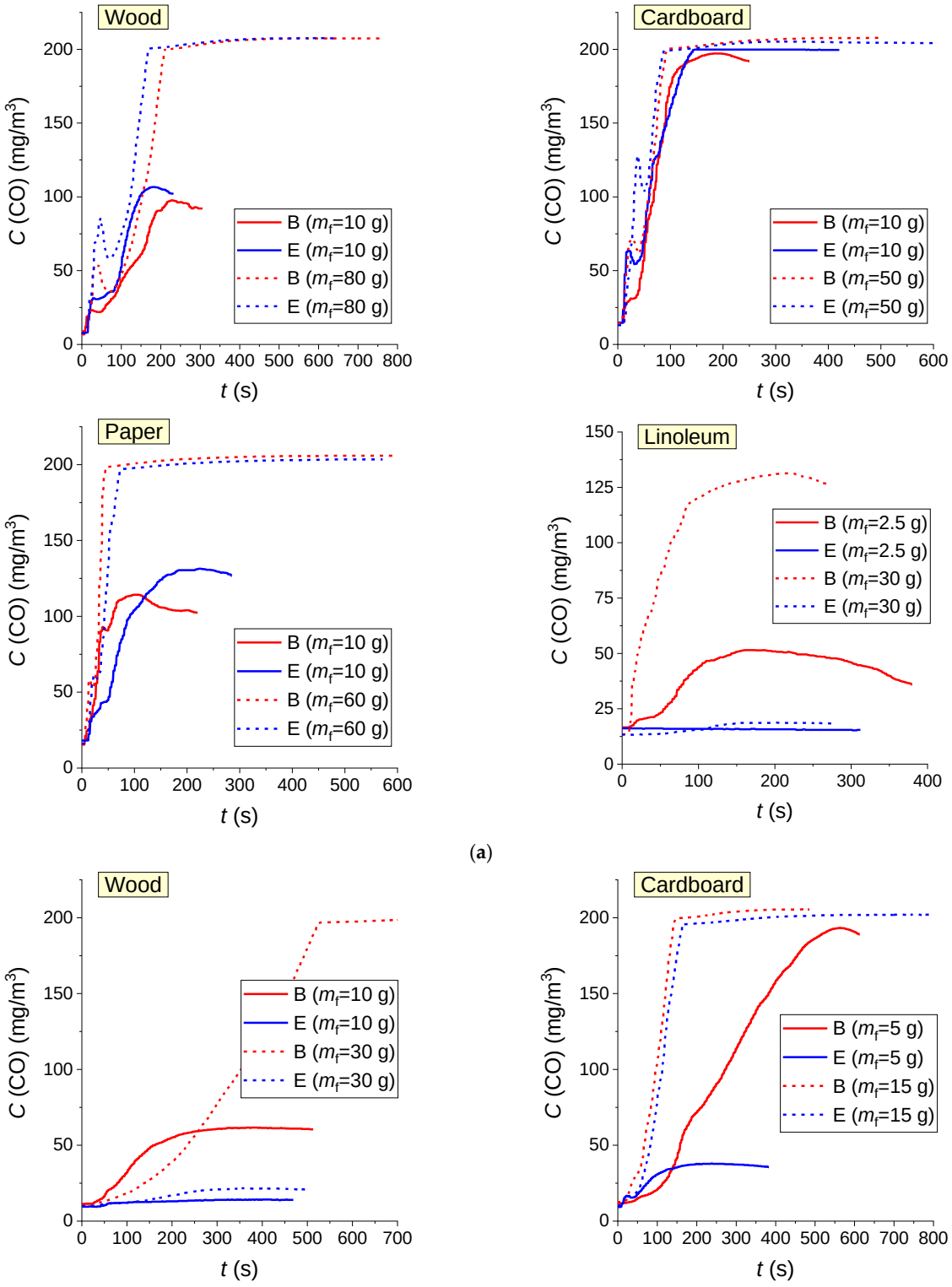

Figure 13. *Cont.*

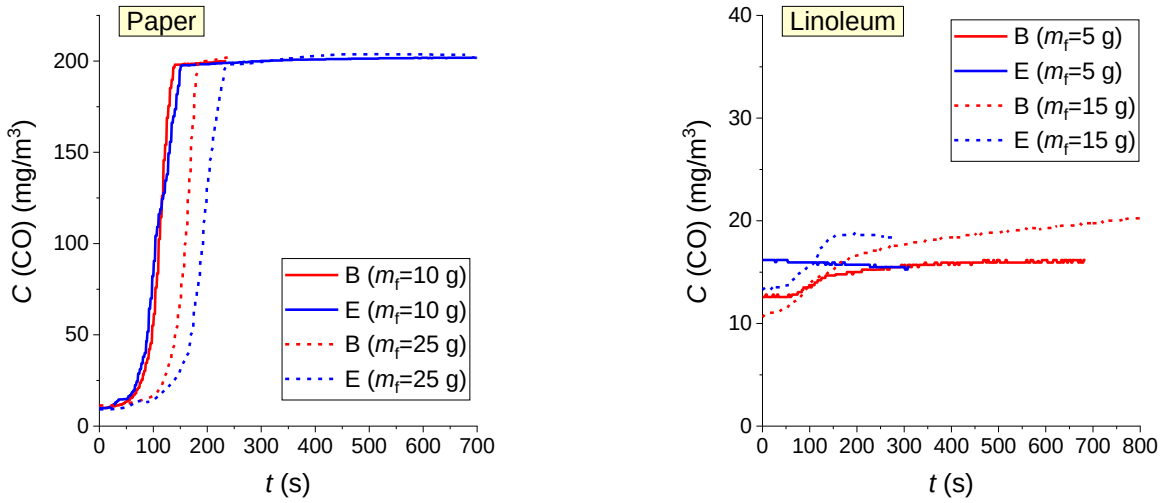

(**b**)

Figure 13. Trends of CO concentrations for the model fires under study when reproducing the conditions of careless handling of fire (gas burner) (**a**) and improper use of heating equipment (hot plate) (**b**), obtained using GDS (B–experimental results for the thermal decomposition of the model fire without suppression; E–experimental results for extinguishing the model fire during thermal decomposition).

Figure 14 presents the trends of O_2, CO, CO_2, H_2 and CH_4 concentrations determined in the experiments for three cases: 1–hot plate heating without aerosol spray; 2–spraying aerosol on the heated surface; 3–spraying aerosol with no heating. Figure 14 demonstrates that the hot plate heating, water mist droplet spraying and evaporation do not affect the GDS sensor readings. This result is necessary to confirm the validity of the data presented in Figure 13.

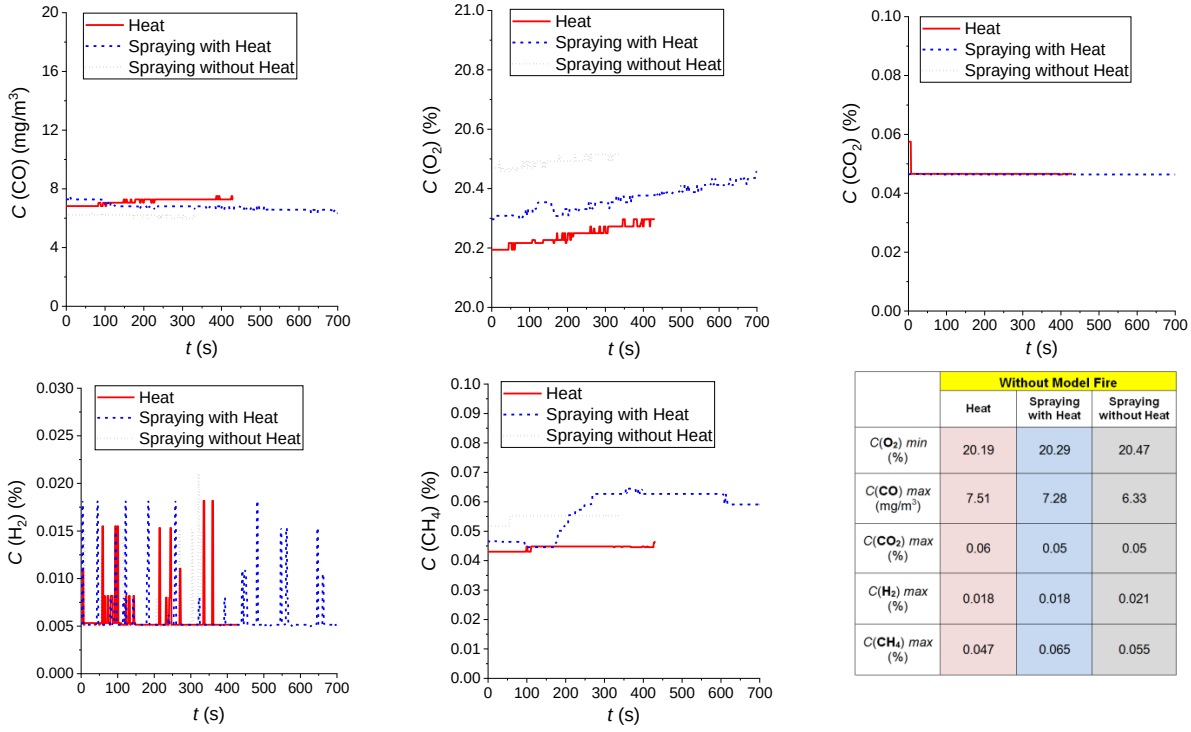

	Without Model Fire		
	Heat	Spraying with Heat	Spraying without Heat
$C(O_2)$ *min* (%)	20.19	20.29	20.47
$C(CO)$ *max* (mg/m^3)	7.51	7.28	6.33
$C(CO_2)$ *max* (%)	0.06	0.05	0.05
$C(H_2)$ *max* (%)	0.018	0.018	0.021
$C(CH_4)$ *max* (%)	0.047	0.065	0.055

Figure 14. Trends of O_2, CO, CO_2, H_2 and CH_4 concentrations: 1–hot plate heating without aerosol spray; 2–spraying aerosol on the heated surface; 3–spraying aerosol with no heating.

Figure 15 presents cumulative histograms of threshold concentrations of gas components (O_2, CO, CO_2, H_2 and CH_4) recorded for all the model fires under study when reproducing the conditions of careless handling of fire (gas burner) and improper use of heating equipment (hot plate). The "normal value" in Figure 15 means the value corresponding to the sensor readings, when there is no pyrolysis of the combustible material.

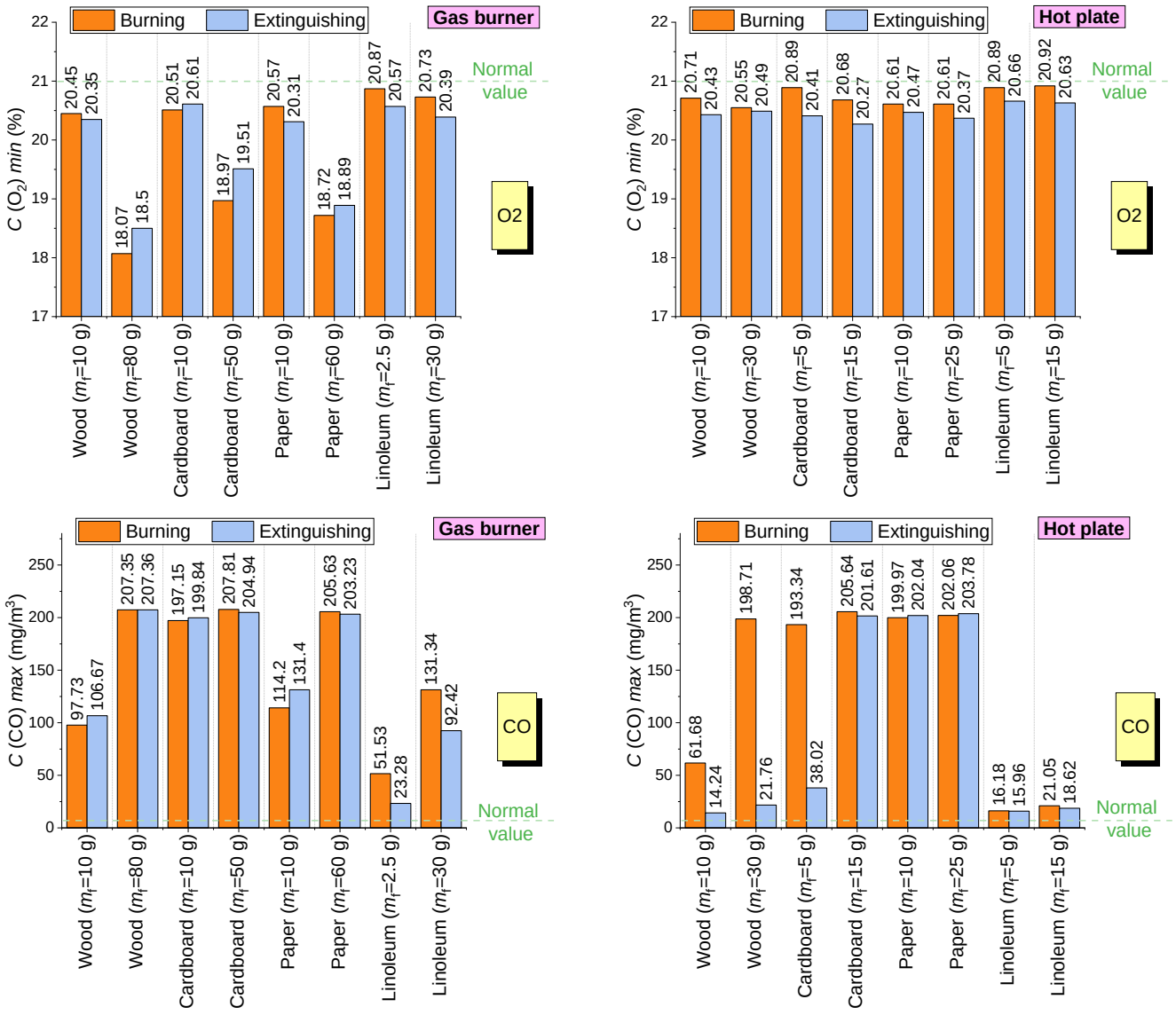

Figure 15. *Cont.*

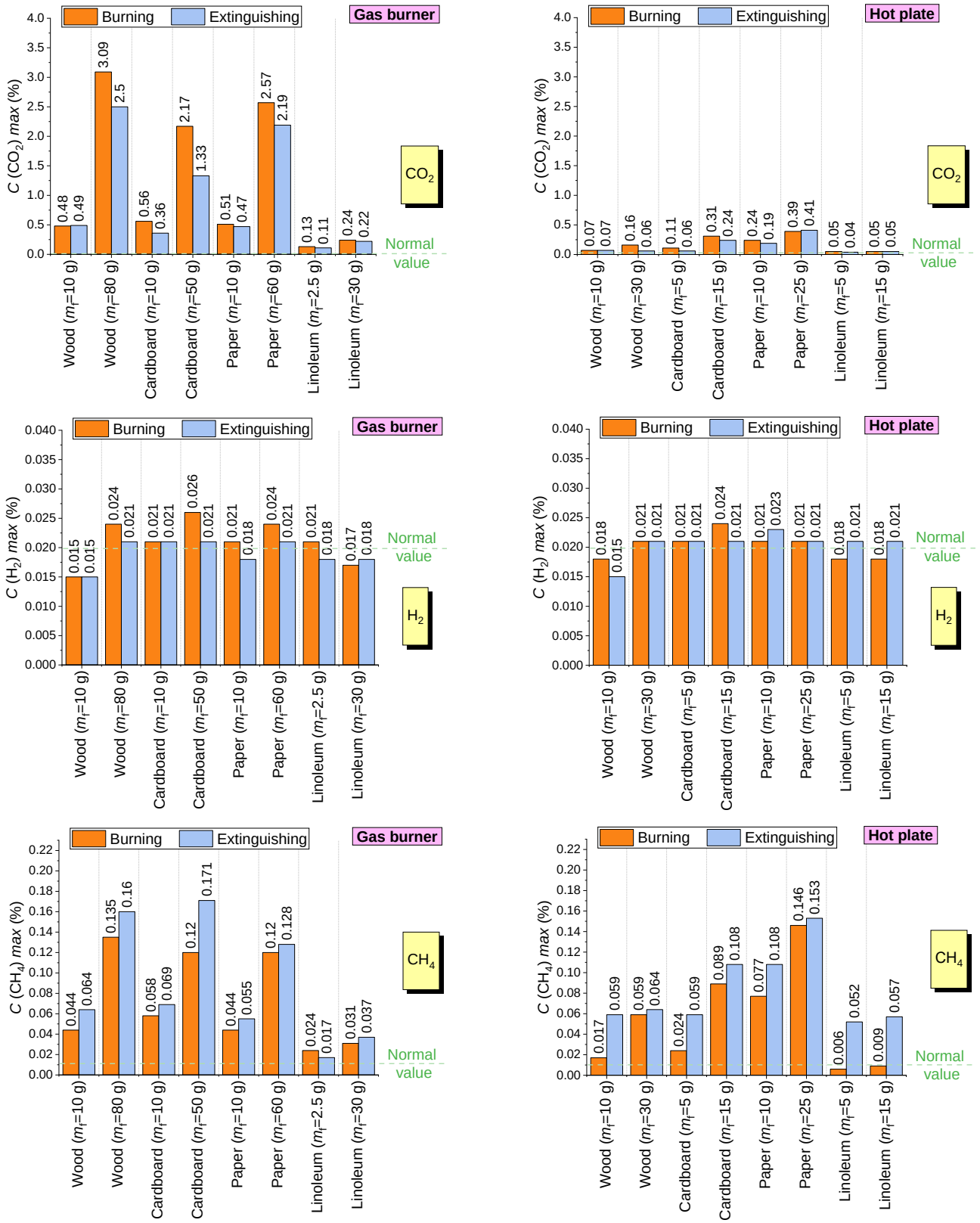

Figure 15. Cumulative histograms of threshold concentrations of gas components (O_2, CO, CO_2, H_2 and CH_4) recorded for all the model fires under study when reproducing the conditions of careless handling of fire (gas burner) and improper use of heating equipment (hot plate) (Burning–experimental results for the thermal decomposition of the model fire without suppression; Extinguishing–experimental results for extinguishing the model fire during thermal decomposition).

Based on the analysis of Figures 13, S1 and S2 (Supplementary Material S), the following key patterns were identified:

- gas burner. CO_2 was found to be highest at the stage of flame combustion. The oxygen concentration here is minimum, which indicates an active oxidation phase. A further decrease in CO_2 concentrations with rising O_2 concentrations indicate that the combustion stage is complete. Constant CO concentrations illustrate the initial moment of smoldering. It was recorded that 40–50 s after ignition, the concentration of O_2 fell from 20.5% to 18.5–20%, whereas the values of CO_2 and CO rose to 0.5–2% and 0.15–0.5%, respectively. The experiments involving GDS revealed that the component concentrations with and without extinguishing the model fire only differ in CO: when a firefighting liquid interacts with the seat of fire, the CO concentration increases to 0.7–1.2%, which indicates a slowdown in the flame combustion and, consequently, smoldering intensification;
- hot plate. Without flame combustion the concentration of O_2 was found (Figure S2) to be 1.5–2% higher than that recorded during flame combustion (Figure S2). The O_2 concentration is higher when the model fire is extinguished than during smoldering when it is not extinguished (which implies the effectiveness of fire suppression). It was also recorded that the interaction of a fire-extinguishing liquid with the seat of fire increases the CO concentration (e.g., for cardboard) compared to the case when there was no fire suppression. This result is consistent with the conclusions drawn from Figure S1.
- The experimental results (Figures 13–15 , S1 and S2) led to some essential conclusions:
- with all the model fires under study, there was no change in H_2 concentrations when the conditions of careless handling of fire (gas burner) and improper use of heating equipment (hot plate) were imitated;
- with the condition reproducing improper use of heating equipment (hot plate), the concentrations of O_2 and CO_2 remain within their normal values and hardly change throughout the experiment (due to the absence of flame combustion of the material);
- the threshold concentrations of such gases as CO, CO_2 and O_2 increase with the growth of the mass of the thermally reacting combustible material;
- the threshold concentrations of CO, CO_2 and O_2 recorded when applying a sprayed aerosol flow to the fire are on average lower than those without any external impact;
- the threshold concentrations of CH_4 recorded when applying a sprayed aerosol flow to the fire are on average higher than those without any external impact;
- the most efficient sensors to detect the moments when combustion and smoldering of combustible materials start and complete are CO and CH_4 sensors.

4.3. Analysis of Experimental Video Recordings

The video recordings of the considered processes, obtained from the VC in the experiments, were processed using the DaVis software. Immediately before the data were uploaded to DaVis, each recording was split into images in the Photron FastcamViewer software, with one image saved per a second. The processing comprised several stages:

- in each image, three horizontal and three vertical profiles of image intensity change were plotted. Intensity is seen as the brightness (luminance) of each separate pixel in the image, which can change in the range of 0–256 counts at 8 bit depth of the VC. Thus, the intensity profile is a set of points, each of them corresponding to the luminance of a separate pixel through which the cross-section passes;
- for each plotted profile, the maximum and minimum intensity values were identified;
- for each image, the arithmetic mean of the minimum intensity was found separately for horizontal and vertical profiles. The same procedure was performed for the maximum intensity;
- for each image, the difference (δ) between the maximum and minimum intensity of horizontal profiles was found. The same procedure was performed for the vertical profiles;

- the curves were plotted for the normalized maximum and minimum intensity values, as well as the difference between them versus time.

There might be sharp fluctuations in the intensity in the course of image processing. These are attributed to the fact that the experimental setup elements such as the window, aluminum beams, etc. are caught on camera. This stresses the necessity of plotting three horizontal and vertical profiles. Figure 16 presents the example of a change in the normalized maximum and minimum intensity values, as well as the difference between them after the model fire was placed on a heating surface (plate).

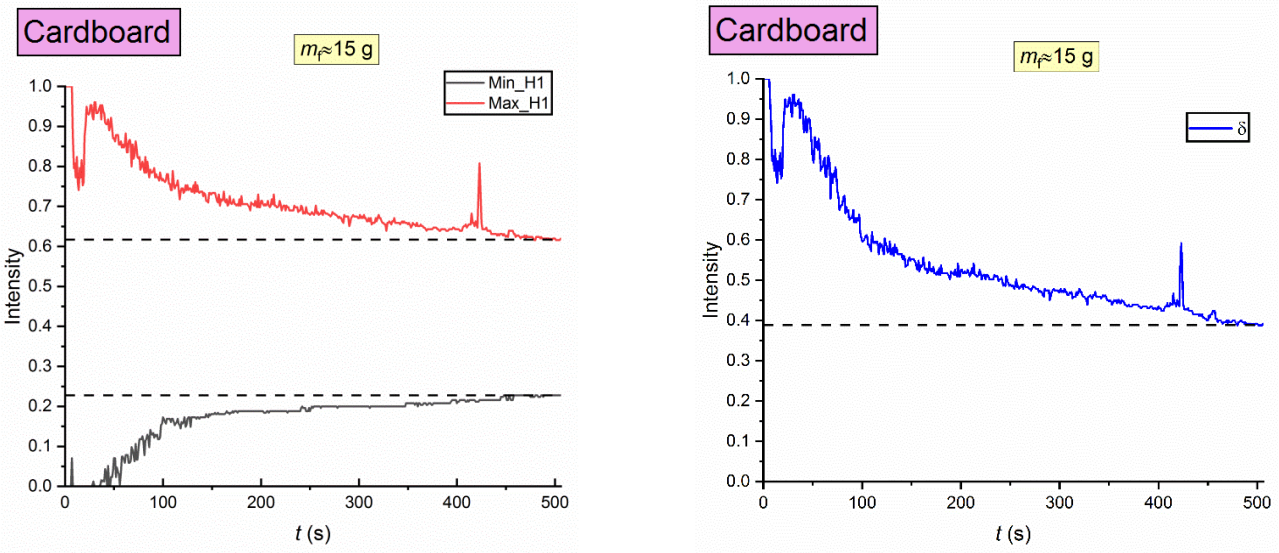

Figure 16. Trends of normalized intensity over time (immediately after placing the model fire made up of cardboard on a hot plate): (**a**) maximum and minimum values (horizontal profiles); (**b**) difference between the maximum and minimum values.

Figure 16 shows a sharp change in the normalized intensity values and in the difference between them when smoke generation begins (after the model fire is placed on a hot surface). The approach in question can be successfully applied to identify the start of smoke generation. The analysis of Figure 16 leads to the conclusion that it is more reasonable to use the difference between the maximum and minimum intensity (δ) to determine the start of smoke generation in rooms, because a change in this parameter reaches 0.6. At the same time, the maximum and minimum intensity within the same time interval (approx. 500 s) changed by no more than 0.4 and 0.25, respectively. Thus, a method involving δ is more sensitive in the image intensity analysis to detect smoke in rooms. Figure 17 shows the example of the change in δ, when reproducing the conditions of improper use of heating equipment for the model fire consisting of wood. In Supplementary Material S, Figures S3–S6 show the parameter δ, when the conditions of improper use of heating equipment were reproduced for the whole group of the model fires under study with their extinguishment. The highlighted areas in Figure 17 correspond to the duration of fire suppression.

Additionally, the average intensity of images obtained from the VC was determined and the corresponding trends were plotted. These are presented in Figure 18 and in Supplementary Material S in Figures S7–S10. The highlighted areas in Figures 18 and S7–S10 correspond to the duration of extinguishing.

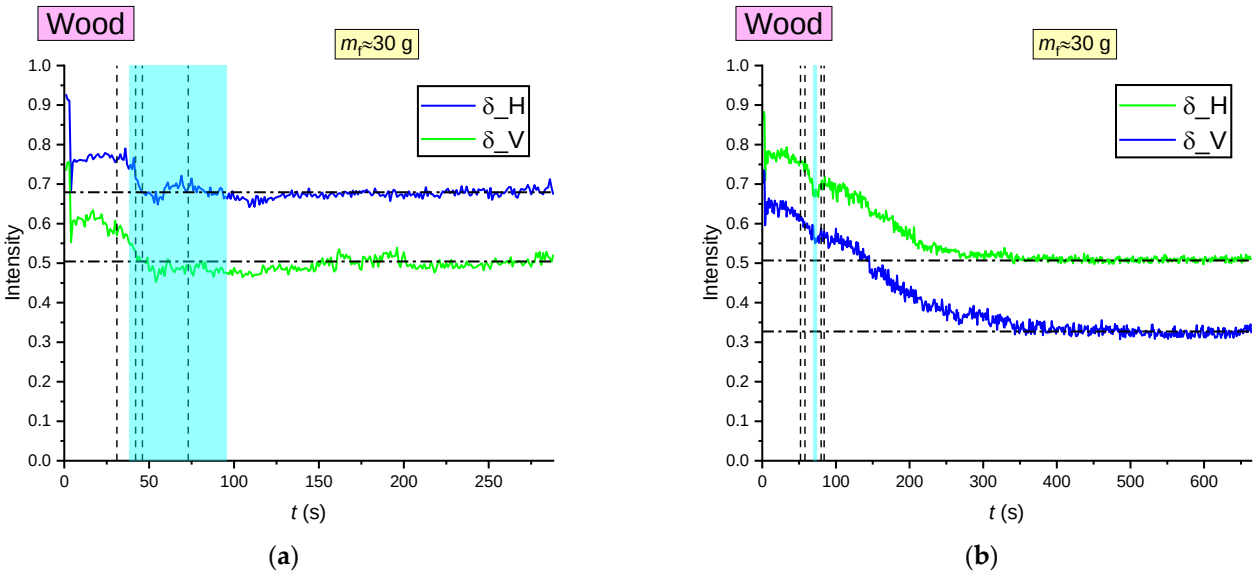

Figure 17. Change in δ when reproducing the conditions of improper use of heating equipment (hot plate) for the model fires consisting of wood with different duration of extinguishment: (**a**) 60 s; (**b**) 5 s.

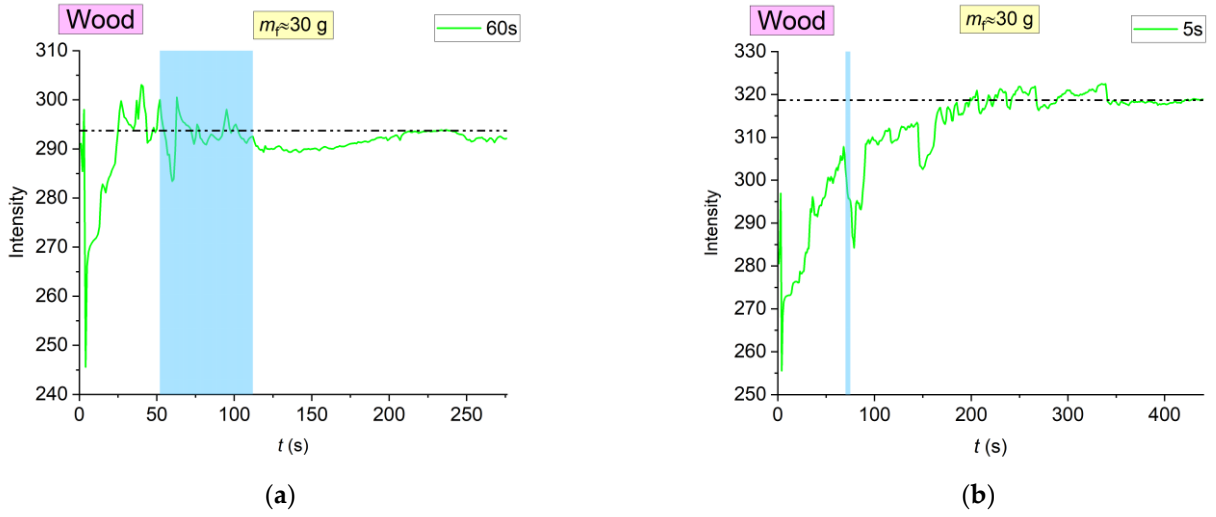

Figure 18. Change in the absolute average intensity of images when reproducing the conditions of improper use of heating equipment (hot plate) for the fires involving wood with different duration of extinguishment: (**a**) 60 s; (**b**) 5 s.

The analysis of experimental data in Figures 17, 18 and S3–S10 revealed the following patterns:

- for model fires involving wood, it is necessary and sufficient to spray water for 30–60 s. With shorter duration of spraying, the average luminous intensity in the image increases after fire suppression completion. This indicates that the flue gas concentrations continue rising. When wood was extinguished, the SD (linear) was not triggered (unlike in the case without fire suppression);
- for model fires involving linoleum, it is sufficient to provide water spraying for 5–10 s. With longer spraying, the time of average image intensity reaching a constant value hardly changes;
- to extinguish model fires involving cardboard, water aerosol should be sprayed for at least 90 s. During extinguishing, combustion intensified a little as a result of fine aerosol discharged on the surface of the reacting material;

- the extinguishing of model fires consisting of paper enhances the smoldering of the combustible material. The aerosol flow generated by the nozzle entrains the oxidizer from the experimental setup space, intensifying the smoldering of this type of fuel. During extinguishing, the average image intensity continues rising, which indicates its low effectiveness.

During the experiments, the effect of water mist on the parameter δ was additionally analyzed. The water mist generated by the humidifier was directed into the experimental setup space and gradually filled it. The images of the inner part of the setup were recorded by the VC and processed using the DaVis software following the algorithm described above. Figure 19 presents the changes in the parameter δ as the setup space is filled with water mist.

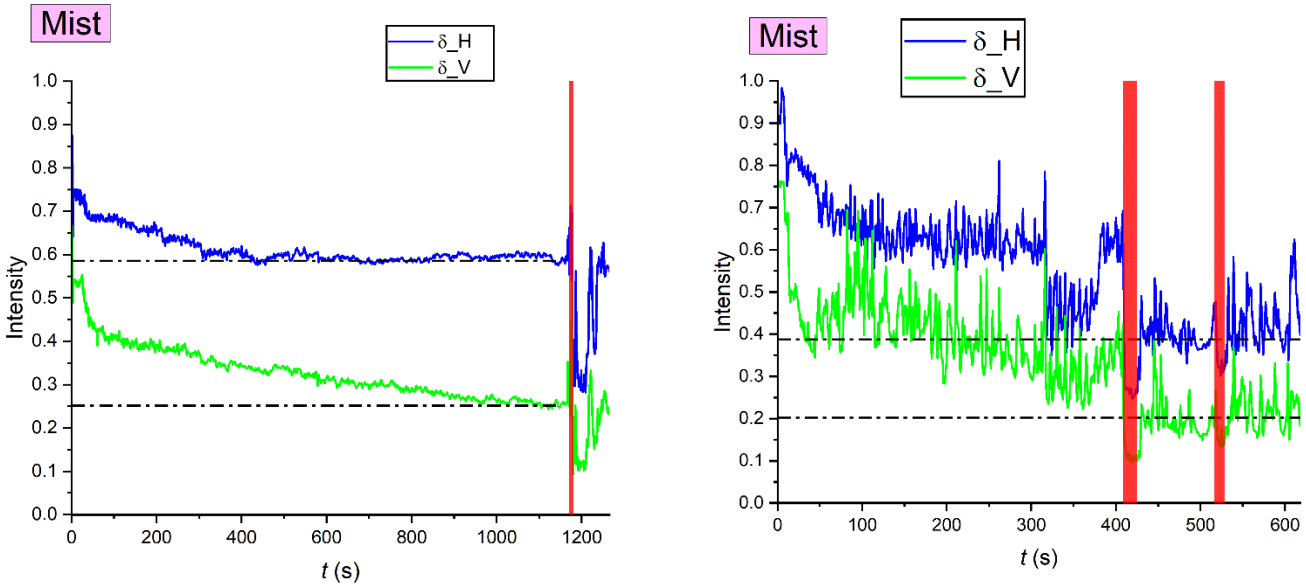

Figure 19. Changes in the parameter δ as the experimental setup space is filled with water mist: (**a**) water mist is released through the lower part of the setup; (**b**) water mist is released through the upper part of the setup.

In Figure 19, the red color denotes the boundaries of time intervals when exhaust ventilation (EV) was switched on. In the first case (Figure 19a), intensity evenly decreased. However, after the exhaust ventilation was turned on, there was a rapid reduction in intensity. It recovered to the original values after a certain period of time. Intensity reduction is accounted for by the fact that once the EV is switched on, the surrounding mist is discharged beyond the setup space. The remaining mist starts circulating inside the experimental setup. Later, the water mist inflow/outflow in the setup stabilizes. After the automatic adjustment of the VC gain, the intensity returns to the previous level. In the second case (when the mist was discharged through the upper part of the setup), fine mist droplets ended up on the protective glass of the camera and circulated near it. This led to a significantly non-monotonic change in the intensity. After the EV was switched on, the intensity fell, as in the first case. Later, the intensity evenly recovered to the previous level. In both cases under study, the maximum reduction in δ was 75–80% for the vertical profiles and 40–60% for the horizontal profiles.

It is an important practical task to scale up the research findings to big fires. Without doubt, it will be necessary to test the physical models developed in this research using full-scale fires as an example. A wide range of publications [47–54] were studied when planning this research. The analysis revealed that two types of fires are commonly used in experimental research: small-sized fires (100 × 100 mm [49], 120 × 120 mm [54], 191 × 279 mm [51]) and large-sized fires (500 × 500 mm [50,53], 600 × 600 mm [48],

900 × 900 mm [52], 960 × 975 mm [47]). Each model fire usually consists of narrow slabs (wooden, plastic, etc.) with a cross-section of 20 × 20 mm to 40 × 40 mm laid at some distance (10–30 mm) from each other in one to six layers [47–54]. Thus, it appears to be common practice to use small-sized fires [47–54]. The research findings [55–58] show that the knowledge of such parameters as specific discharge density, volumetric flow rate of a fire extinguishing liquid [55,58] and extinction time [56] makes it possible to successfully predict (by using the obtained approximation equations) the characteristics of full-scale fire suppression [57,58]. Thus, for instance, the volumes of liquid and time, necessary and sufficient to extinguish fires with an area of up to 1 km ^{2}, were determined using model fires consisting of forest fuels [55,56]. Following the conducted experiments, the threshold conditions that are necessary and sufficient for fire detection using different sensors and systems were determined. One of the main objectives of the research was early fire detection. The fire sizes at this stage normally do not exceed the ones considered in this research and in the other studies [49,51,54]. It is noteworthy that any fire usually starts with a small-sized local ignition. Moreover, in the event of a big fire (characterized by high heat release rate, HRR), all the systems and sensors will be activated with 100% probability. Therefore, the model fire sizes and the heat release corresponding to them are appropriate for accomplishing the objectives of this research. The data obtained from generalizing the research findings make it possible to scale them up to large fires involving typical indoor combustible materials. As regards the heat release from fires, it is common practice [59–61] to use small-sized fires. In reviewing the known studies, the total heat fluxes (convective and radiant heat transfer) of model fires were obtained. They were 18–21 kW/m^2 for wood [59]; 5.3 kW/m^2 for plastic [60]; 11 kW/m^2 for cardboard [61]. The total heat fluxes for model fires used in this research [14] were 15.4–16.6 kW/m^2 for wood and 12.8–13.5 kW/m^2 for cardboard. Thus, the calculated heat fluxes are consistent with the research findings [59,61]. An important parameter of a fire is HRR [52]. According to [62], the HRR corresponds to the heat flux per a unit of the model fire area (specific heat flux). Calculating and determining HRR values is an independent area of study. Within the framework of this study, the main task was to determine the response characteristics of fire detectors, sensors and systems. However, based on the results of [52,61,62], it is possible to recalculate and predict the HRR values for each particular combustion initiation mechanism and each combustible material, respectively. Thus, at known areas of model fires and masses of materials involved, the findings of this study can be approximated to full-scale fires.

A comparison with the results of other studies was performed. Direct comparison of the times and rates of a fire detection is inappropriate due to varying initial conditions of the experiments (model fire characteristics, room type and volume, specific aspects of supply and exhaust ventilation operation, ignition mechanism, type and make of fire detectors, their location, etc.) conducted by different research groups. Nevertheless, the range of times and rates of fire detection were compared. Thus, the findings obtained using the multi-parameter method of fire detection [63] indicate that a smoke detector and CO sensor offer great potential, which is quite consistent with the findings of this research (Figures 11, 12 and 15). The findings [64,65] also illustrate that employing SD and CO sensors can contribute to early fire detection. As noted by Yuan et al. [65], in the case of flame combustion, the most effective detector in terms of the detection rate is FD (t_D < 20 s), which confirms the results of this study (Figure 11a). In other cases, a smoke detector and a CO sensor should be used. With sensors installed immediately above the fire, the average values of t_D were approx. 30 s for SD and 100 s for the CO sensor. With sensors placed further away, the activation delay times were approx. 120 s and 500 s, respectively. This research found that irrespective of the type and mass of combustible material, as well as ignition mechanism, when the sensors and detectors are not above the fire center (Figures 1 and 2), the values of t_D may vary in the range of 20–1000 s for SD and 10–500 s for the CO sensor (at a detection limit of 20 mg/m^3). Thus, the findings of this research are in agreement with those obtained in other studies [63–65].

5. Conclusions

A series of large-scale experiments was conducted in this research. Using the findings, the key characteristics (activation delay times, relative frequency of activation, efficiency factor) of typical fire detectors were determined. Differences in the performance of detectors were identified when simulating different ignition mechanisms with typical indoor combustible materials. The gas analysis and video recording systems were shown to be very effective for fire detection. Below are the key conclusions based on the findings of the conducted research.

- The conducted experiments made it possible to identify the specific aspects of detecting compartment fires with three most common causes: careless handling of fire and failures in electrical networks and heating equipment. To explore the differences in the characteristics of activation of the corresponding sensors in different fire outbreak and development scenarios, a group of materials was used: paper, cardboard, wood and linoleum. An automated system integrating fire (heat, smoke, flame) detectors, contact and non-contact temperature measurement instruments, a gas analysis system and video recording equipment was employed. The evidence from this study suggests that the most valuable information about the course (corresponding stages) of compartment fire suppression is acquired when gas analysis systems, video cameras and heat detectors are used. Each block of sensors has a different response time. Therefore, their combination and certain sequence of activation is crucial to minimize the fire suppression time and liquid consumption.
- Timely triggering of fire suppression system sensors minimized the duration of spraying water and thus its volume. The benefits of the developed combined system turned out to be distinct for each type of fire hazard source and reacting material. In particular, compared to the prescribed water discharge density [66] (in the range of 0.08–0.12 L/(m^2s) at a maximum duration of water application of no less than 30–60 min), which reaches 144–432 L/m^2, the discharge density necessary to suppress a fire when using the proposed approach based on the conducted research is 8.7 L/m^2 for wood; 0.9 L/m^2 for linoleum; 3.6 L/m^2 for paper; and 7.2 L/m^2 for cardboard (15–30 times as low). The water discharge density was calculated by multiplying the specific discharge density of the FMT–100 nozzle ($\psi \approx 0.03$ L/(m^2s)) by the spraying time (time of fire suppression).
- One of the major tasks of fire suppression systems is to provide the control of the process to optimize the consumption of extinguishing agents and reduce the time of extinguishment and property damage. The presented results of the experiments with a water discharge system turned on indicate that it is generally possible to optimize the extinguishment time and liquid volume with all the types of materials and fire hazard sources. The minimum sufficient times of water spraying at fixed discharge density were determined. These data can be used to predict the necessary conditions for different surface areas of materials, taking the available spraying system characteristics into account. The conducted experiments revealed that a combined gas analysis and video recording system can be efficiently used to determine the reaction stage and material type. This information allows optimizing a fire-fighting agent consumption and the time of fire containment. The timely detection of fire outbreaks is a key factor in the efficient containment and suppression of fires.

Supplementary Materials: The following supporting information can be downloaded at: https://www.mdpi.com/article/10.3390/fire5050155/s1, Supplementary Material A: Video of model fire (wood) when reproducing conditions of unsafe operation of heating equipment (hot plate) without extinguishing; Supplementary Material B: Video of model fire (wood) when reproducing conditions of unsafe operation of heating equipment (hot plate) with extinguishing; Supplementary Material C: Video of model fire (paper) when reproducing conditions of unsafe operation of heating equipment (hot plate) without extinguishing; Supplementary Material D: Video of model fire (paper) when reproducing conditions of unsafe operation of heating equipment (hot plate) with extinguishing; Supplementary Material E: Video of model fire (cardboard) when reproducing conditions of unsafe operation of heating equipment (hot plate) without extinguishing; Supplementary Material F: Video of model fire (cardboard) when reproducing conditions of unsafe operation of heating equipment (hot plate) with extinguishing; Supplementary Material G: Video of model fire (linoleum) when reproducing conditions of unsafe operation of heating equipment (hot plate) without extinguishing; Supplementary Material H: Video of model fire (linoleum) when reproducing conditions of unsafe operation of heating equipment (hot plate) with extinguishing; Figure S1: Trends of O_2, CO, CO_2, H_2 and CH_4 concentrations obtained using GDS for the model fires under study when imitating the conditions of careless handling of fire (gas burner), and threshold concentrations of gas components (B—burning; E—extinguishing): a—wood; b—cardboard; c—paper; d—linoleum; Figure S2: Trends of O_2, CO, CO_2, H_2 and CH_4 concentrations obtained using GDS for the model fires under study when imitating the conditions of improper use of heating equipment (hot plate), and threshold concentrations of gas components (B—burning; E—extinguishing): a—wood; b—cardboard; c—paper; d—linoleum; Figure S3: Change in δ when reproducing the conditions of improper use of heating equipment (hot plate) for the model fires consisting of wood with different duration of extinguishment: a—90 s; b—60 s; c—30 s; d—15 s; e—5 s; Figure S4: Change in δ when reproducing the conditions of improper use of heating equipment (hot plate) for the model fires consisting of linoleum with different duration of extinguishment: a—60 s; b—30 s; c—15 s; d—10 s; e—5 s; Figure S5: Change in δ when reproducing the conditions of improper use of heating equipment (hot plate) for the model fires consisting of cardboard with different duration of extinguishment: a—120 s; b—90 s; c—60 s; d—30 s; Figure S6: Change in δ when reproducing the conditions of improper use of heating equipment (hot plate) for the model fires consisting of paper with different duration of extinguishment: a—90 s; b—30 s; Figure S7: Change in the absolute average intensity of images when reproducing the conditions of improper use of heating equipment (hot plate) for the fires involving wood with different duration of extinguishment: a—90 s; b—60 s; c—30 s; d—15 s; e—5 s; Figure S8: Change in δ when reproducing the conditions of improper use of heating equipment (hot plate) for model fires consisting of linoleum with different duration of extinguishment: a—30 s; b—15 s; c—10 s; d—5 s; Figure S9: Change in δ when reproducing the conditions of improper use of heating equipment (hot plate) for the fires consisting of cardboard with different duration of extinguishment: a—120 s; b—90 s; c—60 s; d—30 s; Figure S10: Change in δ when reproducing the conditions of improper use of heating equipment (hot plate) for the fires consisting of paper with different duration of extinguishment: a—90 s; b—30 s.

Author Contributions: G.K.—conceptualization, funding acquisition; R.V.—Planning and conducting experiments; A.S.—Conducting pilot studies; A.Z.—Writing—Original draft preparation of manuscript. All authors have read and agreed to the published version of the manuscript.

Funding: The Research was supported by the Russian Science Foundation (project No. 21-19-00009, https://rscf.ru/en/project/21-19-00009/, accessed on 1 July 2022).

Conflicts of Interest: The authors declare no conflict of interest.

Nomenclature

$C(CH_4)$	mass concentration of methane in the gas–vapor mixture, %
$C(CO)$	mass concentration of carbon monoxide in the gas–vapor mixture, mg/m^3
$C(CO_2)$	mass concentration of carbon dioxide in the gas–vapor mixture, %
$C(H_2)$	mass concentration of hydrogen in the gas–vapor mixture, %
$C(O_2)$	mass concentration of oxygen in the gas–vapor mixture, %
I_0	output current of welder inverter, A
I	average image intensity, normalized to the maximum value
j	number of experiments in a set
m_f	mass of burning materials, g
n_a	number of sensors of a particular type, activated in the experiment
n_D	total number of sensors of a particular type in the experiment
P	overall relative frequency of activation of each sensor type;
$P_1, P_2, \ldots, P_j$	relative frequency of sensor activation in each experiment, %
S_f	area of the seat of fire, cm^2
t	time, s
t_D	fire detector response delay time, s
$t_{D(min)}$	minimum fire detector activation delay, recorded in the experiments, s
t_f	model fire suppression time, s
T	temperature, °C
T_f	model fire surface temperature, °C
T_s	hot plate surface temperature, °C.
Greek	
α	fire detector efficiency factor
δ	difference between the maximum and minimum values of normalized image intensity in the plotted cross-section
ψ	specific discharge density, l/(m^2·s).
Abbreviations	
DAIM	digital and analog input module
EV	exhaust ventilation
FACD	fire alarm control device
FD	flame detector
GDS	gas detection system
HD	heat detector
PC	personal computer
PPU	pyrometer processor unit
PSE	pyrometer sensing element
SD	smoke detector
SV	supply ventilation
TC	thermocouple
VC	video camera
FAC	fire alarm circuit.

References

1. Festag, S. The statistical effectiveness of fire protection measures: Learning from real fires in Germany. *Fire Technol.* **2021**, *57*, 1589–1609. [CrossRef]
2. Himoto, K. Conceptual framework for quantifying fire resilience—A new perspective on fire safety performance of buildings. *Fire Saf. J.* **2021**, *120*, 103052. [CrossRef]
3. Sheng, D.; Deng, J.; Zhang, W.; Cai, J.; Zhao, W.; Xiang, J. A statistical image feature-based deep belief network for fire detection. *Complexity* **2021**, *2021*, 5554316. [CrossRef]
4. Bonner, M.; Wegrzynski, W.; Papis, B.K.; Rein, G. KRESNIK: A top-down, statistical approach to understand the fire performance of building facades using standard test data. *Build. Environ.* **2020**, *169*, 106540. [CrossRef]
5. Russian Emergency Situations Ministry. FGBU VNII GOChS (FTs) State Report "On the State of Protection of the Population and Territories of the Russian Federation from Natural and Man-Made Emergencies in 2020"; Moscow, 2021. Available online: https://www.mchs.gov.ru/dokumenty/5946?ysclid=l8ml4n4a4r289814793 (accessed on 1 July 2022).
6. Dai, H.; Wang, X.; Chen, X.; Nan, X.; Hu, Y.; He, S.; Yuan, B.; Zhao, Q.; Dong, Z.; Yang, P. Suppression characteristics of double-layer wire mesh on wheat dust flame. *Powder Technol.* **2020**, *360*, 231–240. [CrossRef]

7. Singh, P.P.; Sabnani, C.S.; Kapse, V.S. Hotspot analysis of structure fires in urban agglomeration: A case of Nagpur City, India. *Fire* **2021**, *4*, 38. [CrossRef]
8. Quiroz, N.F.; Walls, R.; Cicione, A. Towards understanding fire causes in informal settlements based on inhabitant risk perception. *Fire* **2021**, *4*, 39. [CrossRef]
9. Park, J.; Kwark, J. Experimental study on fire sources for full-scale fire testing of simple sprinkler systems installed in multiplexes. *Fire* **2021**, *4*, 8. [CrossRef]
10. Kuznetsov, G.V.; Kropotova, S.S.; Voytkov, I.S.; Strizhak, P.A. Influence of the component composition of extinguishing fluids on the droplet distribution in an aerosol cloud. *Powder Technol.* **2022**, *395*, 838–849. [CrossRef]
11. Hung, H.Y.; Lin, C.Y.; Chuang, Y.J.; Luan, C.P. Application development of smoke leakage test apparatus for door sets in the field. *Fire* **2022**, *5*, 12. [CrossRef]
12. Liu, H.; Cordeiro, I.M.D.C.; Yuen, A.C.Y.; Chan, Q.N.; Kook, S.; Yeoh, G.H. Application of multi-parametric characterization to water-based fire suppression systems in compartment fire scenarios. *Numer. Heat Transf. Part A Appl.* **2022**, 1–19. [CrossRef]
13. Festag, S. Analysis of the effectiveness of the smoke alarm obligation—Experiences from practice. *Fire Saf. J.* **2021**, *119*, 103263. [CrossRef]
14. Zhdanova, A.; Volkov, R.; Sviridenko, A.; Kuznetsov, G.; Strizhak, P. Influence of compartment fire behavior at ignition and combustion development stages on the operation of fire detectors. *Fire* **2022**, *5*, 84. [CrossRef]
15. Qiu, X.; Xi, T.; Sun, D.; Zhang, E.; Li, C.; Peng, Y.; Wei, J.; Wang, G. Fire detection algorithm combined with image processing and flame emission spectroscopy. *Fire Technol.* **2018**, *54*, 1249–1263. [CrossRef]
16. Elangovan, M.; Prakash, D.S.; Hemadri, C. Development of toxic gas monitoring and alarm system. In *Advances in Design and Thermal Systems*; Lecture Notes in Mechanical Engineering; Springer: Singapore, 2021; pp. 39–48. [CrossRef]
17. Le Maoult, Y.; Sentenac, T.; Orteu, J.J.; Arcens, J.P. A new approach based on a low cost CCD camera in the near infrared. *Process Saf. Environ. Prot.* **2007**, *85*, 193–206. [CrossRef]
18. Foggia, P.; Saggese, A.; Vento, M. Real-time fire detection for video-surveillance applications using a combination of experts based on color, shape, and motion. *IEEE Trans. Circuits Syst. Video Technol.* **2015**, *25*, 1545–1556. [CrossRef]
19. Kou, L.; Wang, X.; Guo, X.; Zhu, J.; Zhang, H. Deep learning based inverse model for building fire source location and intensity estimation. *Fire Saf. J.* **2021**, *121*, 103310. [CrossRef]
20. Nauman, Z.; Iqbal, S.; Khan, M.I.; Tahir, M. WSN-based fire detection and escape system with multi-modal feedback. In *International Conference on Multimedia Communications, Services and Security*; Springer: Berlin/Heidelberg, Germany, 2011; Volume 149 CCIS, pp. 251–260. [CrossRef]
21. Huang, Y.; Zhou, X.; Cao, B.; Yang, L. Computational fluid dynamics-assisted smoke control system design for solving fire uncertainty in buildings. *Indoor Built Environ.* **2020**, *29*, 40–53. [CrossRef]
22. Bello, R.; Sama, B.A.; Gambo, N.; Ahijo, Y.M. Design analysis and implementation of automatic fire extinguishing system using ATmega16 microcontroller as control. *Asian J. Res. Rev. Phys.* **2021**. [CrossRef]
23. Zhang, L.; Wang, G. Design and Implementation of Automatic Fire Alarm System Based on Wireless Sensor Networks. In Proceedings of the 2009 International Symposium on Information Processing (ISIP'09), Huangshan, China, 21–23 August 2009.
24. Liao, X.B.; Shan, H.Q.; Quan, Z.Z.; Peng, L. The design and implementation of automatic fire extinguishing and explosion suppression system's testing equipment. In *Applied Mechanics and Materials*; Scientific.Net: Baech, Switzerland, 2014.
25. Tang, Z.; Xu, G.; Yang, S.; Deng, J.; Xu, Q.; Chang, P. Fire-retardant foam designed to control the spontaneous combustion and the fire of coal: Flame retardant and extinguishing properties. *Powder Technol.* **2021**, *384*, 258–266. [CrossRef]
26. Voytkov, I.S.; Kuznetsov, G.V.; Strizhak, P.A. The critical atomization conditions of high-potential fire suppressant droplets in an air flow. *Powder Technol.* **2021**, *384*, 505–521. [CrossRef]
27. Sheng, Y.; Peng, Y.; Yan, C.; Li, Y.; Ma, L.; Wang, Q.; Zhang, S. Influence of nanoparticles on rheological properties and foam properties of mixed solutions of fluorocarbon and hydrocarbon surfactants. *Powder Technol.* **2022**, *398*, 117067. [CrossRef]
28. Kelesidis, G.A.; Kholghy, M.R.; Zuercher, J.; Robertz, J.; Allemann, M.; Duric, A.; Pratsinis, S.E. Light scattering from nanoparticle agglomerates. *Powder Technol.* **2020**, *365*, 52–59. [CrossRef]
29. Wehbe, R.; Shahrour, I. A BIM-based smart system for fire evacuation. *Future Internet* **2021**, *13*, 221. [CrossRef]
30. Mukherjee, A.; Shome, S.K.; Bhattacharjee, P. Survey on internet of things based intelligent wireless sensor network for fire detection system in building. In *Smart Innovation, Systems and Technologies*; Springer: Berlin/Heidelberg, Germany, 2022.
31. GOST 12.1.007-76 Occupational Safety Standards System (SSBT). Harmful Substances. Classification and General Safety Requirements (with Amendments No. 1, 2), GOST Dated March 10, 1976 No. 12.1.007-76. 2021. Available online: https://npopris.ru/wp-content/uploads/2015/03/%D0%93%D0%9E%D0%A1%D0%A2-12.1.007-76.pdf (accessed on 1 July 2022).
32. SP 12.13130.2009 Definition of Categories of Premises, Buildings and Outdoor Installations in Terms of Explosion and Fire Hazard (with Amendment No. 1). 2021. Available online: http://fire-consult.ru/wp-content/catalog-files/sp_mchs/sp_12.13130.2009.pdf?ysclid=l8mpwu6mss5617760 (accessed on 1 July 2022).
33. Almanasra, S.; Alshahrani, A. Alternative real-time image-based smoke detection algorithm. *Adv. Sci. Technol. Eng. Syst.* **2020**, *5*, 123–128. [CrossRef]
34. Ge, L.; Shao, Y.; Wang, Y.; Zhang, G.; Zhang, Z.; Liu, L. Experimental research on inerting characteristics of carbon dioxide used for fire extinguishment in a large sealed space. *Process Saf. Environ. Prot.* **2020**, *142*, 174–190. [CrossRef]

35. Xiong, C.; Wang, Z.; Huang, Y.; Shi, F.; Huang, X. Smart evaluation of building fire scenario and hazard by attenuation of alarm sound field. *J. Build. Eng.* **2022**, *51*, 104264. [CrossRef]
36. Hao, H.; Chow, C.L.; Lau, D. Effect of heat flux on combustion of different wood species. *Fuel* **2020**, *278*, 118325. [CrossRef]
37. Diab, M.T.; Haelssig, J.B.; Pegg, M.J. The behaviour of wood crib fires under free burning and fire whirl conditions. *Fire Saf. J.* **2020**, *112*, 102941. [CrossRef]
38. Bluvshtein, N.; Villacorta, E.; Li, C.; Hagen, B.C.; Frette, V.; Rudich, Y. Early detection of smoldering in silos: Organic material emissions as precursors. *Fire Saf. J.* **2020**, *114*, 103009. [CrossRef]
39. Vershinina, K.Y.; Dorokhov, V.V.; Romanov, D.S.; Strizhak, P.A. Combustion stages of waste-derived blends burned as pellets, layers, and droplets of slurry. *Energy* **2022**, *251*, 123897. [CrossRef]
40. Vershinina, K.; Dorokhov, V.; Romanov, D.; Strizhak, P. Ignition, combustion, and mechanical properties of briquettes from coal slime and oil waste, biomass, peat and starch. *Waste Biomass Valorization* **2022**, 1–15. [CrossRef]
41. Yang, S.; Nie, W.; Lv, S.; Liu, Z.; Peng, H.; Ma, X.; Cai, P.; Xu, C. Effects of spraying pressure and installation angle of nozzles on atomization characteristics of external spraying system at a fully-mechanized mining face. *Powder Technol.* **2019**, *343*, 754–764. [CrossRef]
42. Chvanov, S.V.; Kuznetsov, G.V.; Strizhak, P.A.; Volkov, R.S. The necessary water discharge density to suppress fires in premises. *Powder Technol.* **2022**, *408*, 117707. [CrossRef]
43. Volkov, R.S.; Kopylov, N.P.; Kuznetsov, G.V.; Khasanov, I.R. Experimental investigation of the suppression of crown and ground forest fires. *J. Eng. Phys. Thermophys.* **2019**, *92*, 1453–1465. [CrossRef]
44. Antonov, D.V.; Volkov, R.S.; Voitkov, I.S.; Zhdanova, A.O.; Kuznetsov, G.V. Influence of special additives in a water aerosol on the suppression of a forest fire with it. *J. Eng. Phys. Thermophys.* **2018**, *91*, 1250–1259. [CrossRef]
45. Strizhak, P.A.; Volkov, R.S. The integral characteristics of the deceleration and entrainment of water droplets by the counter flow of high-temperature combustion products. *Exp. Therm. Fluid Sci.* **2016**, *75*, 54–65. [CrossRef]
46. Volkov, R.S.; Kuznetsov, G.V.; Strizhak, P.A. Criterion expressions for conditions and deceleration and subsequent entrainment of water drops by high-temperature gases. *Tech. Phys.* **2015**, *60*, 1310–1315. [CrossRef]
47. Arvidson, M. Large-scale water spray and water mist fire suppression system tests for the protection of ro-ro cargo decks on ships. *Fire Technol.* **2014**, *50*, 589–610. [CrossRef]
48. Li, Y.Z.; Ingason, H. Parametric study of design fires for tunnels with water-based fire suppression systems. *Fire Saf. J.* **2021**, *120*, 103107. [CrossRef]
49. Yimin, L.; Yao, B.; Qin, J. Preliminary burning tests on PVC fires with water mist. *Polym. Test.* **2005**, *24*, 583–587. [CrossRef]
50. Yao, B.; Cong, B.H.; Qin, J.; Chow, W.K. Experimental study of suppressing Poly(methyl methacrylate) fires using water mists. *Fire Saf. J.* **2012**, *47*, 32–39. [CrossRef]
51. Tamanin, F. A Study of the extinguishment of vertical wood slabs in self-sustained burning by water spray application. *Combust. Sci. Technol.* **1976**, *14*, 1–15. [CrossRef]
52. Noaki, M.; Delichatsios, M.A.; Yamaguchi, J.; Ohmiya, Y. Heat release rate of wooden cribs with water application for fire suppression. *Fire Saf. J.* **2018**, *95*, 170–179. [CrossRef]
53. Rappsilber, T.; Below, P.; Krüger, S. Wood crib fire tests to evaluate the influence of extinguishing media and jet type on extinguishing performance at close range. *Fire Saf. J.* **2019**, *106*, 136–145. [CrossRef]
54. Pancawardani, F.; Arini, D.; Yunindar, R.P.; Ramadhan, M.L.; Imran, F.A.; Nugroho, Y.S. Analysis of water mist fire suppression system applied on cellulose fire. *Procedia Eng.* **2017**, *170*, 344–351. [CrossRef]
55. Volkov, R.S.; Zhdanova, A.O.; Kuznetsov, G.V.; Strizhak, P.A. Determination of the volume of water for suppressing the thermal decomposition of forest combustibles. *J. Eng. Phys. Thermophys.* **2017**, *90*, 789–796. [CrossRef]
56. Volkov, R.S.; Zhdanova, A.O.; Kuznetsov, G.V.; Strizhak, P.A. Suppression of the thermal decomposition reaction of forest combustible materials in large-area fires. *J. Eng. Phys. Thermophys.* **2018**, *91*, 411–419. [CrossRef]
57. Volkov, R.S.; Kuznetsov, G.V.; Strizhak, P.A. Experimental study of the suppression of flaming combustion and thermal decomposition of model ground and crown forest fires. *Combust. Explos. Shock Waves* **2017**, *53*, 678–688. [CrossRef]
58. Volkov, R.S.; Kuznetsov, G.V.; Strizhak, P.A. Suppression of flaming combustion and thermal decomposition of condensed matter at different heights of the beginning of water array motion. *Combust. Explos. Shock Waves* **2020**, *56*, 83–91. [CrossRef]
59. Horvat, A.; Sinai, Y.; Pearson, A.; Most, J.M. Contribution to flashover modelling: Development of a validated numerical model for ignition of non-contiguous wood samples. *Fire Saf. J.* **2009**, *44*, 779–788. [CrossRef]
60. Terrei, L.; Acem, Z.; Marchetti, V.; Lardet, P.; Boulet, P.; Parent, G. In-depth wood temperature measurement using embedded thin wire thermocouples in cone calorimeter tests. *Int. J. Therm. Sci.* **2021**, *162*, 106686. [CrossRef]
61. He, Q.; Liu, N.; Xie, X.; Zhang, L.; Zhang, Y.; Yan, W. Experimental study on fire spread over discrete fuel bed-part I: Effects of packing ratio. *Fire Saf. J.* **2021**, *126*, 103470. [CrossRef]
62. ISO 5660-1:2015 "Reaction-to-Fire Tests—Heat Release, Smoke Production and Mass Lose Rate—Part 1: Heat Release Rate (Cone Calorimeter Method) and Smoke Production Rate (Dynamic Measurement)", IDT; 2015. Available online: https://standartgost.ru/g/ISO_5660-1:2015?ysclid=l8mqe6j1ot821538227 (accessed on 1 July 2022).
63. Qu, N.; Li, Z.; Li, X.; Zhang, S.; Zheng, T. Multi-parameter fire detection method based on feature depth extraction and stacking ensemble learning model. *Fire Saf. J.* **2022**, *128*, 103541. [CrossRef]

64. Baek, J.; Alhindi, T.J.; Jeong, Y.S.; Jeong, M.K.; Seo, S.; Kang, J.; Shim, W.; Heo, Y. Real-time fire detection system based on dynamic time warping of multichannel sensor networks. *Fire Saf. J.* **2021**, *123*, 103364. [CrossRef]
65. Yuan, L.; Thomas, R.A.; Rowland, J.H.; Zhou, L. Early fire detection for underground diesel fuel storage areas. *Process Saf. Environ. Prot.* **2018**, *119*, 69–74. [CrossRef]
66. SP 485.1311500.2020 Fire Protection Systems. Automatic Fire Extinguishing Installations. Design Code of 31 August 2020. Available online: https://docs.cntd.ru/document/573004280?ysclid=l8mqhv577123503754 (accessed on 1 July 2022). (In Russian).